NASA MEMO 3-10-59L

NASA

MEMORANDUM

JET EFFECTS ON THE BASE PRESSURE OF A CYLINDRICAL AFTERBODY WITH MULTIPLE-JET EXITS

By William R. Scott and Travis H. Slocumb, Jr.

Langley Research Center
Langley Field, Va.

Declassified April 23, 1962

NATIONAL AERONAUTICS AND SPACE ADMINISTRATION
WASHINGTON
April 1959

NATIONAL AERONAUTICS AND SPACE ADMINISTRATION

MEMORANDUM 3-10-59L

JET EFFECTS ON THE BASE PRESSURE OF A CYLINDRICAL AFTERBODY WITH MULTIPLE-JET EXITS*

By William R. Scott and Travis H. Slocumb, Jr.

SUMMARY

A wind-tunnel investigation to determine the effects of multiple-jet exits on the base pressure of a cylindrical afterbody has been conducted at Mach numbers from 0.6 to 1.4. The number of jets has been varied from one to six; the diameter of the convergent nozzles has also been varied. Jet total-pressure ratio ranged up to approximately 10.

The results show that the jet total-pressure ratio at which peak negative pressures occur on the base decreased as the ratio of jet diameter to base diameter was increased; increasing jet area by increasing the number of jets at constant diameter also resulted in a shift of the peak negative pressure toward lower jet total-pressure ratios. With three or more jets symmetrically arranged on the base, a region of super-ambient pressure was found near the center of the base region at high jet total-pressure ratios.

INTRODUCTION

Recent interest in missile configurations in which several propulsive jets discharge from a common cylindrical base has given rise to a need for a systematic study of the base-pressure characteristics of such configurations. For the single-jet case, extensive data are currently available (e.g., refs. 1 and 2), but for multiple-jet configurations, only meager data have been published. The investigations of references 3 and 4 present data for tests of twin-jet configurations and those of references 5 and 6 are concerned with specific multijet configurations.

In the present investigation, pressures were measured across the base of a cylindrical afterbody with one to six sonic nozzles discharging

*Title, Unclassified.

parallel to the body axis at jet total-pressure ratios from 1 to approximately 10. The ratio of jet diameter to base diameter of these nozzles (designated jet-to-base diameter ratio herein) was varied from 0.155 to 0.450. With the exception of the six-nozzle configuration, the center lines of the multiple-jet nozzles were displaced 22 percent of the body diameter from the body axis.

This investigation is part of a general program in progress in the Internal Aerodynamics Branch of the Langley Research Center to study the effects of propulsive jets on the base drag of bluff afterbodies at transonic speeds. The free-stream Mach number ranged from 0.6 to 1.4. The Reynolds number varied from 3.3 to 4.4 $\times 10^6$ per foot. The boundary layer approaching the base was fully turbulent and all these tests were conducted at zero angle of attack.

SYMBOLS

A	area
$C_{p,b}$	base pressure coefficient, $\frac{p_b - p_\infty}{q_\infty}$
d	diameter
H	total pressure
M	free-stream Mach number
p	static pressure
q	dynamic pressure

Subscripts:

b	base
j	jet
∞	free stream

APPARATUS

The general arrangement of the setup utilized in this investigation is shown in figure 1. The top and bottom walls of the $4\frac{1}{2}$- by $4\frac{1}{2}$-inch

test section had four longitudinal slots with a ratio of open area to total area of 1 to 8. Details of the slot geometry and the Mach number distribution along the test section are presented in reference 7. A centrifugal blower supplied air to the test section through a 30-inch-diameter duct at a maximum stagnation pressure of approximately 2 atmospheres at a stagnation temperature of 250° F. The air was returned to atmosphere through a diffuser with an area ratio of 1.75 to 1. Mach number control through the subsonic range was effected by varying the free-stream stagnation pressure. In order to reach supersonic Mach numbers, the static pressure in the test section was reduced by applying suction to the plenum chamber which surrounds the test section.

The model support consisted of a 1-inch-diameter steel tube cantilevered from the tunnel approach duct as shown in figure 1. The jet air, which was supplied to the models through the support tube, was stored in outside tanks at atmospheric temperature and a pressure of 310 lb/sq in. A pneumatically operated valve placed in the air supply pipe upstream of the tunnel was utilized to vary the total pressure of the jets.

A total of 13 models were tested in this investigation. The models were grouped according to the number of jets and a photograph of representative models of each group tested is shown in figure 2. Bell-mouthed nozzles were machined in cylindrical metal plugs which were soldered flush with the end of the model support tube. A table of the models tested in this investigation is also shown in figure 2. For the single-jet models, the nozzles were positioned in the center of the cylindrical plug, and for the two-, three-, and four-jet models the nozzles were spaced symmetrically at a constant radius of 0.22 inch from the center line of the plug. The nozzles were spaced at a radius of 0.28 inch from the center line for the six-jet model. The static-pressure orifice locations on the model base are also indicated in figure 2 and tabulated in table I.

The tunnel was instrumented to measure the free-stream stagnation pressure and temperature in the 30-inch-diameter supply duct and the free-stream static pressure in the plenum chamber. The pressures measured on the base of the models and the total pressure of the jet, which was measured upstream in the supply pipe, were fed into transducers and continuously recorded on pen-trace potentiometers. A double-pass coincidence schlieren system with a spark duration of 6 microseconds was utilized in photographing the flow field of the models.

Precision

With an instrument accuracy of ±0.5 percent for the pressure transducers and pen-trace potentiometers, the maximum errors in the base

pressure coefficients are estimated to be ±0.005 throughout the Mach number range. Disturbances associated with tunnel blockage are considered negligible; these data are therefore presented without correction for tunnel-wall interference.

RESULTS AND DISCUSSION

The basic results of this investigation are presented in figures 3 to 7 where the base pressure coefficient is plotted as a function of the jet total-pressure ratio. The free-stream Mach number is indicated for each test condition in the upper left-hand corner of each of the six sets of curves. The curves at each Mach number represent the pressures measured at the orifice locations on the base of the cylindrical afterbody. Since there was a wide variation in the pressures measured at the different orifice locations on the base of the three-, four-, and six-jet models, an area-weighted average of the pressures was also calculated for these models and is shown as a dashed curve in figures 5 to 7. The base area of the models was divided into two regions by straight lines connecting the jet axes. The center-line pressure was multiplied by the closed area and the rim pressure by the outer area to obtain an area-weighted average. For the two configurations in which base pressures were measured at more than these two stations, the added pressures were neglected in computing the average in order that the results might be compared directly with those obtained with the more limited instrumentation. The error thus introduced is negligible even though the orifice between nozzles indicated lower pressures, since the area represented by this orifice was very small. These data figures are grouped according to the number of nozzles, and parts (d) of figures 3 to 6 present a corresponding set of schlieren photographs.

Effect of Jet Total-Pressure Ratio

Single jets.- The effect of jet total-pressure ratio on the base pressure coefficient of the single-jet nozzles is shown in figures 3(a), 3(b), and 3(c) for jet-to-base diameter ratios of 0.225, 0.320, and 0.450, respectively.

In general, the base pressure coefficient becomes increasingly negative as the jet pressure ratio increases above the no-flow condition and reaches maximum negative values which, for the larger jets only, occur within the range of these tests. The slope of these curves increased as the jet-to-base diameter ratio is increased and reached a peak value which with increasing jet size occurred at progressively lower jet total-pressure ratios. With the diameter ratio of 0.450, the base pressure

coefficient increases with jet total-pressure ratio after the peak negative pressure is reached.

For all these configurations the variation of the base pressure coefficient with the jet total-pressure ratio fall into typical patterns which are dependent upon the free-stream Mach number. At jet total-pressure ratios below that corresponding to the peak negative base pressure coefficient, the base pressure is predominately influenced by mixing along the jet boundary; thus, with increasing jet diameter, the pumping effectiveness of the jet is increased and the curve has a higher slope. At jet total-pressure ratios above those corresponding to the peak negative value of the base pressure coefficient, the interference of the jet with the external flow in the region of the base is the prominent factor; the pressure ratio at which the peak negative base pressure coefficient occurs is therefore lower for the larger diameter jets. The initial reflex in the curves in figure 3(c) which differs from the usual pattern seen in the previous figures takes place near the design pressure ratio of the sonic nozzle and was also reported in reference 1.

Schlieren photographs of the flow in the base region of the single-jet model are presented in figure 3(d). The free-stream Mach numbers are indicated below each group of photographs and the jet total-pressure ratio is indicated at the lower left-hand corner of each photograph. At the top of each column, the jet-to-base diameter ratio is given.

Two jets.- The effect of jet total-pressure ratio on the base pressure coefficient of the two-jet nozzles is shown in figures 4(a) to 4(c). For these models, the jet-to-base diameter ratios of the individual nozzles were 0.155, 0.225, and 0.320. Comparison with the single-jet data previously discussed shows marked similarity in trends although the absolute values differ. Other two-jet data, reference 8, indicate that with supersonic nozzles (jet Mach number of 2.5) of equal exit area, the base pressure at subsonic Mach numbers and at these jet total-pressure ratios was considerably less than that indicated by this sonic nozzle data.

Schlieren photographs of the two-jet models are presented in figure 4(d).

Three jets.- The effect of jet total-pressure ratio on the base pressure coefficient of the three-jet nozzles is shown in figures 5(a) to 5(c). These nozzles were symmetrically spaced with their center lines on a circle whose radius was 0.22 inch from the center line of the afterbody. As with the two-jet configurations, the jet-to-base diameter ratios were 0.155, 0.225, and 0.320. Because the pressure at the base orifices differed substantially, an area-weighted average is plotted as a dashed curve in these figures. Again, for the small-diameter

jets, as in the preceding plots, the curves form the familiar pattern as the jet total pressure is increased. The irregularities in the static pressure at the two orifice locations in figures 5(b) and 5(c) result from the interaction of the three jets with themselves and the external flow. In figure 5(c), with the large jet-to-base diameter ratio, the inboard static orifice, although covering a small area, measured positive base pressures above a jet total-pressure ratio of 5. Although not plotted in this figure, the measured positive base pressure coefficients approached large values as indicated by the trend of the faired curves; however, the average weighted curve shows that the effect due to the positive pressures was not large. Schlieren photographs of these models are presented in figure 5(d).

Four jets.- The effect of jet total-pressure ratio on the base pressure coefficient of the four-jet models is shown in figures 6(a) to 6(c). These models had jet-to-base diameter ratios of 0.155, 0.225, and 0.278. In figure 6(a), with the diameter ratio of 0.155, the pressure coefficients differ considerably at the two orifice locations on the base; again, the dashed curve is the area-weighted average of the base pressure. With the diameter ratio of 0.225, figure 6(b), the difference in base pressure coefficient between the two base orifice locations reached a maximum of 0.5 at a Mach number of 0.6 and jet total-pressure ratio of 5.

The largest jet-to-base diameter ratio for the four-jet models was 0.278. Four orifices were arranged on a radial line extending between two of the jets. (See table I for static-pressure orifice locations.) The pressure coefficients on the base of this model are shown in figure 6(c). There is a substantial variation of the base pressure coefficients at the four orifice locations up to $M = 1.0$. Above a jet total-pressure ratio of 6 at $M = 1.2$ to 1.4, the base pressure coefficient recorded in the center region was higher than the other three base pressure locations and positive base pressure coefficients would have resulted if the jet total-pressure ratio had been increased further. For the larger jets the peak negative pressure at supersonic Mach numbers occurred at a jet total-pressure ratio of approximately 4.

Six jets.- The effect of jet total-pressure ratio on the base pressure coefficient of the six-jet model is shown in figure 7. The jet-to-base diameter ratio was 0.225. It can be seen from the sketch at the top of figure 7 and in figure 2 that two orifices were located in the center area, one was placed between two of the jet exits, and a fourth was located on the outside rim of the model. The dashed curve is an area-weighted average of the orifice locations. The large variations in the base pressure coefficient at a free-stream Mach number of 0.6 results from a high pumping effectiveness of the jets in lowering the base pressure. At the lowest jet total-pressure ratios the mixing along the jet boundaries results in more or less uniform aspiration of the

base region. With increasing pressure ratio, the jets expand externally and interfere with each other and with the wake boundary; since the interference effects are nonuniform, they lead to wide variations in pressure at the different orifice locations.

Effect of Mutual Jet Interference

To explain the pressure buildup at the center of the three-, four-, and six-jet models, a three-jet model with a jet-to-base diameter ratio of 0.320 was tested, and static pressures were measured at 10 locations on the base. The schematic drawing in figure 8(a) shows three jets exhausting at overpressure. The reverse flow of the jet air originating from the point of intersection of the jets is indicated by the heavy arrow pointing toward the base of the model at the center line. The arrows pointing radially from the center of the model base represent this high-pressure air from the center region exhausting radially between adjacent jets.

The amount of influence that the interference effect has on the base pressure coefficient on the center section of the model base is a function of the proximity of the point of mutual interference to the base. As the point of interference moves closer to the base, the base pressure increases. This effect can be accomplished by increasing the diameter of the jets or by increasing the jet total-pressure ratio and free-stream Mach number. Since there exists a high-pressure region at the center of the model base and a low-pressure region outside of the area confined by the three nozzles, the high-pressure air tends to flow through the space between the three nozzles into the low-pressure region. Figure 8(b) presents the base pressure coefficients at each orifice location for a free-stream Mach number of 1.4 and total jet-pressure ratio of 10.5. For these test conditions radial jet Mach numbers of approximately 0.9 were reached at the pressure orifice locations between the propulsive jets.

Effect of Number of Jets

Superimposing curves from figures 3 to 7 on a single set of coordinates emphasizes the effect of varying the number of jets. Typical plots taken from tests of one to six jets of equal jet-to-base diameter ratio for each jet (0.225) are shown in figure 9. These curves emphasize the shift in minimum base pressure coefficient toward higher jet total-pressure ratios as the number of jets decrease. This shift is readily explained on a basis of the decrease in the interference between the jet and wake boundaries as the number of jets decreased; therefore, a higher jet total-pressure ratio is required for the favorable interference

to overcome the pumping effect of the jets. This also accounts for the reversal of the order of the curves at high jet total-pressure ratios.

These data may be similarly compared as a function of Mach number at constant jet total-pressure ratios and this type of comparison has been found more convenient. Accordingly, a more detailed comparison on this basis is presented in figures 10 and 11. In evaluating the influence of number of jets, an attempt has been made to separate the effects of change in jet area and change in jet periphery. Because both are linear functions of the number of jets if the jet diameter is constant, the data are first compared on this basis in figure 10. A second comparison is based upon constant jet area where the diameter of the individual jets decreases as the number of jets increase. Since the area of the individual jet varies as the square of the diameter, and the periphery varies as the first power, increasing the number of jets while holding the total area constant leads to increased jet periphery. This comparison is presented in figure 11.

Constant-diameter jets (variable area).- Base pressure coefficients obtained with one to four jets whose diameter was held constant are plotted in figure 10. As the jet-to-base diameter ratio was held constant, the total jet exit area varies directly with the number of jets.

For the models tested, free-stream Mach number had very little effect on the base pressure coefficient at a jet total-pressure ratio of 2. At the higher jet total-pressure ratios, the effect of Mach number was more pronounced and the curves were usually well separated.

Peak negative base pressure coefficients occurred in the transonic speed range for all the jet configurations. At supersonic speeds, an increase in the base pressure coefficient resulted and is attributed to the pressure rise associated with the stronger trailing shock waves caused by the turning of the free-stream flow away from the base of the models by the jet flow. (See schlieren photographs of figs. 5(d) and 6(d).)

The variation of the base pressure coefficient with number of jets in figure 10 shows no well-defined trends; however, at jet total-pressure ratios of 2, 4, and 6, the four-jet configuration usually had the lowest base pressure coefficient throughout the Mach number range. (See figs. 10(a) and 10(b).) For the large jet-to-base diameter ratio (0.320) at a jet total-pressure ratio of 10, the opposite effect was noted in figure 10(c) where a large increase in the base pressure coefficient occurred with increasing number of jets.

Constant-area jets (variable diameter).- In figure 11 the total jet exit area was kept constant by decreasing the jet diameters as the

number of jets were increased. Again, base pressure coefficient is plotted against free-stream Mach number. These configurations would have the same amount of thrust regardless of the number of jets for a given set of conditions.

These curves show no well-defined variation in base pressure due to increasing the number of jets. The overall spread between the curves when compared on a basis of constant total jet area is however much less than that observed in the constant-diameter comparisons of figure 10. The agreement of the base pressure coefficient for different numbers of jets was substantially better for the smaller jets (fig. 11(a)) than for the larger jets (fig. 11(b)).

Within the limits of ±15 percent, the base pressure coefficient was independent of number of jets when compared on the constant-total-area basis, whereas differences of two to three times this magnitude were observed in other comparisons. This suggests that the designer confronted with lack of data on clustered jet configurations may, for a preliminary estimate, use data obtained in tests of single-jet configurations of equal total jet area for the case where the jet area is less than 20 percent of the cross-sectional area of the afterbody.

Effect of Jet-To-Base Diameter Ratio

The contour curves in figure 12 present $C_{p,b}$ as a function of d_j/d_b and H_j/p_∞ at free-stream Mach numbers of 0.9 and 1.4. Curves are presented for the one-, two-, three-, and four-jet models. These curves were obtained by cross-plotting the data in figures 3 to 7.

Inspection of the curves in figure 12 shows a small band of minimum base pressure coefficients extending from left to right with a decreasing negative slope. Below and to the left of this band, mixing along the jet boundary exerts the major influence and controls the variation of the pressure on the model base. Above and to the right of the minimum-base-pressure band, the dominating effect is the impinging of the jet boundary on the free-stream wake. The pumping effectiveness of the jet is a function of the jet periphery and the rate of discharge. Therefore, in the region of the curve where mixing is the dominant parameter, the base pressure coefficient at constant jet total-pressure ratios decreases as the jet-to-base diameter ratio increases since both the jet periphery and the mass flow increase. Similarly, at constant jet-to-base diameter ratios, the base pressure coefficient decreases as the jet total-pressure ratio increases because the mass of air issued by the jet and the velocity along the jet boundary increase. Above the band of minimum base pressure coefficients where the favorable interference effect of the

jets is predominant, the base pressure coefficient increases with increasing jet-to-base diameter ratio and jet total-pressure ratio.

As the number of jets increases (figs. 12(b) to 12(d)), there is little change in the general trend of the curves except that the minimum-base-pressure-coefficient band occurs at smaller jet-to-base diameter ratios. Attention is drawn to the change in the ordinate scale which for the single-jet curve (fig. 12(a)) extends to 0.7, while for the other parts of figure 12 it is terminated at 0.32 and 0.36. From these curves, it can be seen that the minimum base pressure coefficients for all configurations are approximately the same for a given free-stream Mach number. The values of the minimum base pressure coefficients are -0.45 at $M = 0.9$ and -0.35 at $M = 1.4$. The ratio of the minimum base pressure coefficients at these Mach numbers approximates the inverse ratio of the dynamic pressures corresponding to the Mach numbers; however, this relationship is not general in that it fails to apply at intermediate Mach numbers.

CONCLUSIONS

From the transonic tunnel tests of the effects of propulsive multiple jets on base pressure of a cylindrical afterbody, the following conclusions are drawn:

1. With the number of jets held constant, the peak negative base pressures occur at lower jet total-pressure ratios as the jet-to-base diameter ratio increases.

2. At constant jet-to-base diameter ratios, the jet total-pressure ratio at which the peak negative base pressure occurs decreases with increasing number of jets.

3. It is possible to obtain relatively high pressures in the center of the base region of a multiple-jet configuration if the jet exits are placed so that a mutual jet interference occurs close to the afterbody base.

4. For total jet areas less than 20 percent of the cross-sectional area of the afterbody, the base pressure may for preliminary estimates be considered independent of the number of jets.

Langley Research Center,
National Aeronautics and Space Administration,
Langley Field, Va., December 30, 1958.

REFERENCES

1. Cubbage, James M., Jr.: Jet Effects on Base and Afterbody Pressures of a Cylindrical Afterbody at Transonic Speeds. NACA RM L56C21, 1956.

2. Baughman, L. Eugene, and Kochendorfer, Fred D.: Jet Effects on Base Pressures of Conical Afterbodies at Mach 1.91 and 3.12. NACA RM E57E06, 1957.

3. Salmi, Reino J., and Klann, John L.: Investigation of Boattail and Base Pressures of Twin-Jet Afterbodies at Mach Number 1.91. NACA RM E55C01, 1955.

4. Leiss, Abraham: Free-Flight Investigation of Effects of Simulated Sonic Turbojet Exhaust on the Drag of Twin-Jet Boattail Bodies at Transonic Speeds. NACA RM L56D30, 1956.

5. Baughman, L. Eugene: Wind-Tunnel Investigation at Mach 1.9 of Multijet-Missile Base Pressures. NACA RM E54L14, 1955.

6. Knapp, Ronald J., and Johnson, Wallace E.: Flight Measurements of Pressures on Base and Rear Part of Fuselage of the Bell X-1 Research Airplane at Transonic Speeds, Including Power Effects. NACA RM L52L01, 1953.

7. Nelson, William J., and Cubbage, James M., Jr.: Effects of Slot Location and Geometry on the Flow in a Square Tunnel at Transonic Mach Numbers. NACA RM L53J09, 1953.

8. Nelson, William J., and Scott, William R.: Jet Effects on the Base Drag of a Cylindrical Afterbody With Extended Nozzles. NACA RM L58A27, 1958.

TABLE I

STATIC-PRESSURE ORIFICE LOCATIONS ON MODEL BASE

Number of jets	d_j/d_b	Number and arrangement of orifices	Radial distance of each orifice from center of model base, in.			
			Orifice			
			1	2	3	4
1	0.225, 0.320, and 0.450	Two orifices on radial lines 90° apart	0.345	0.345		
2	0.155, 0.225, and 0.320	Two orifices on a radial line	0	0.345		
3	0.155, 0.225, and 0.320	Two orifices on a radial line	0	0.345		
4	0.155 and 0.225	Two orifices on a radial line	0	0.345		
	0.278	Four orifices on a radial line	0	0.160	0.280	0.40
6	0.225	Four orifices on a radial line	0	0.120	0.240	0.360

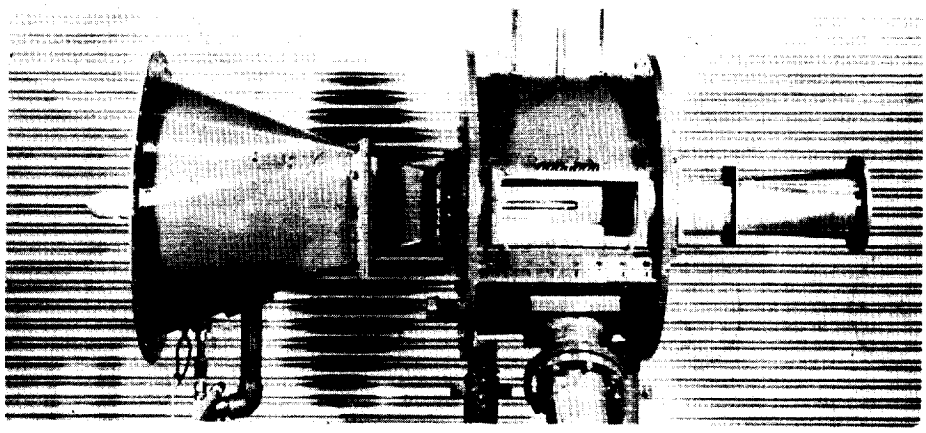

L-59-156

(a) $4\frac{1}{2}$- by $4\frac{1}{2}$-inch slotted test section.

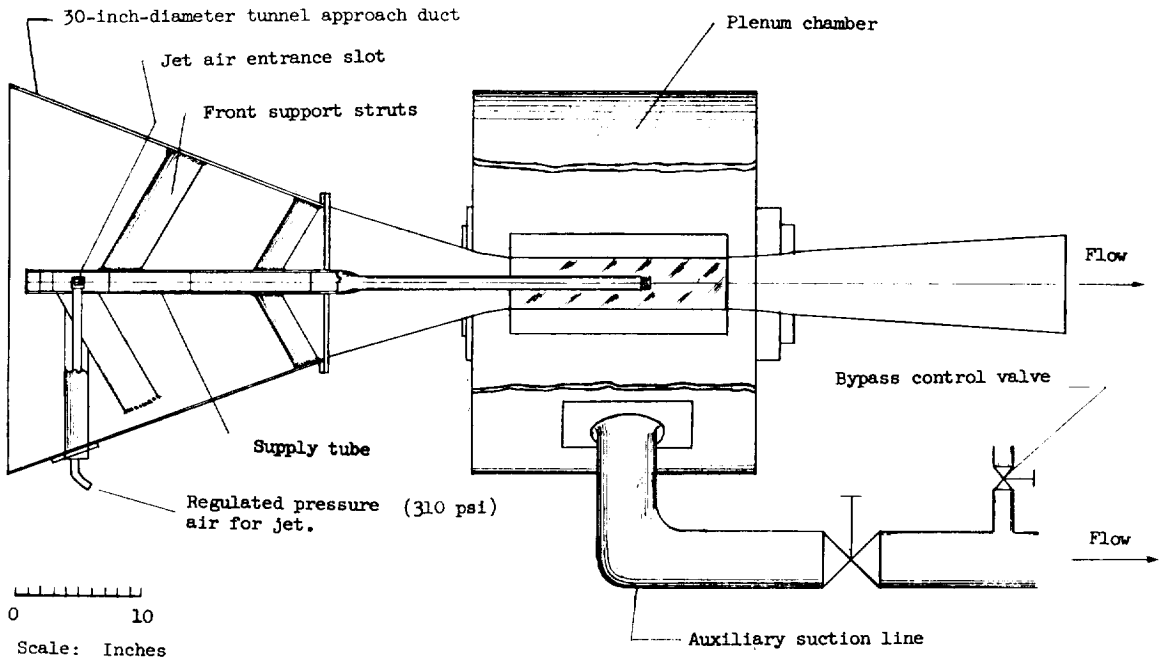

(b) Sketch of tunnel showing ducting for jet flow.

Figure 1.- Tunnel and sting support.

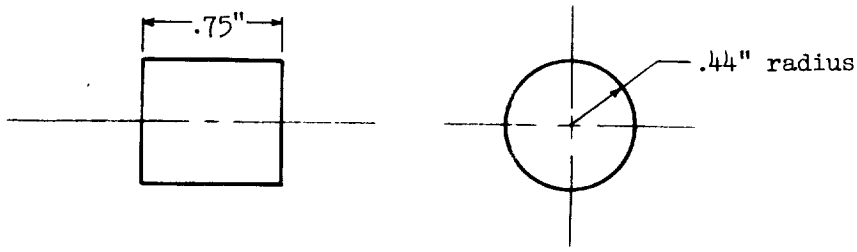

Cylindrical metal plug

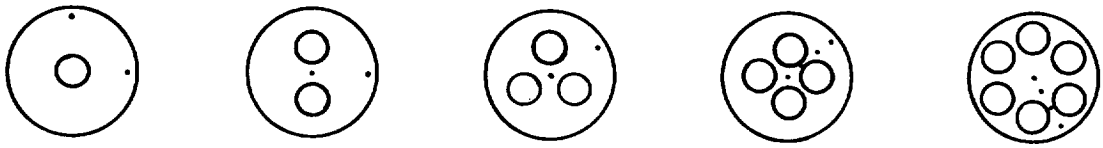

Representative models of each group

Table of models tested

*d_j/d_b	1 jet	2 jets	3 jets	4 jets	6 jets
0.155		x	x	x	
.225	x	x	x	x	x
.278				x	
.320	x	x	x		
.450	x				

*d_j/d_b of each jet.

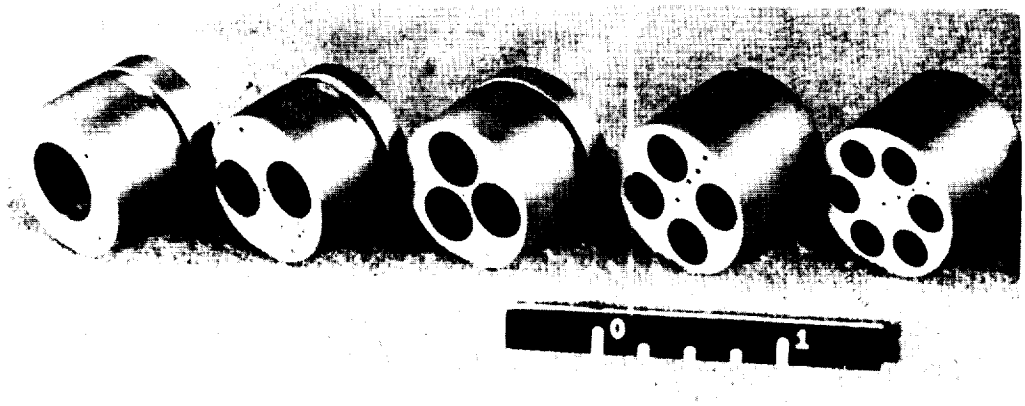

L-59-157

Figure 2.- Tabulation of model parameters and photograph of models.

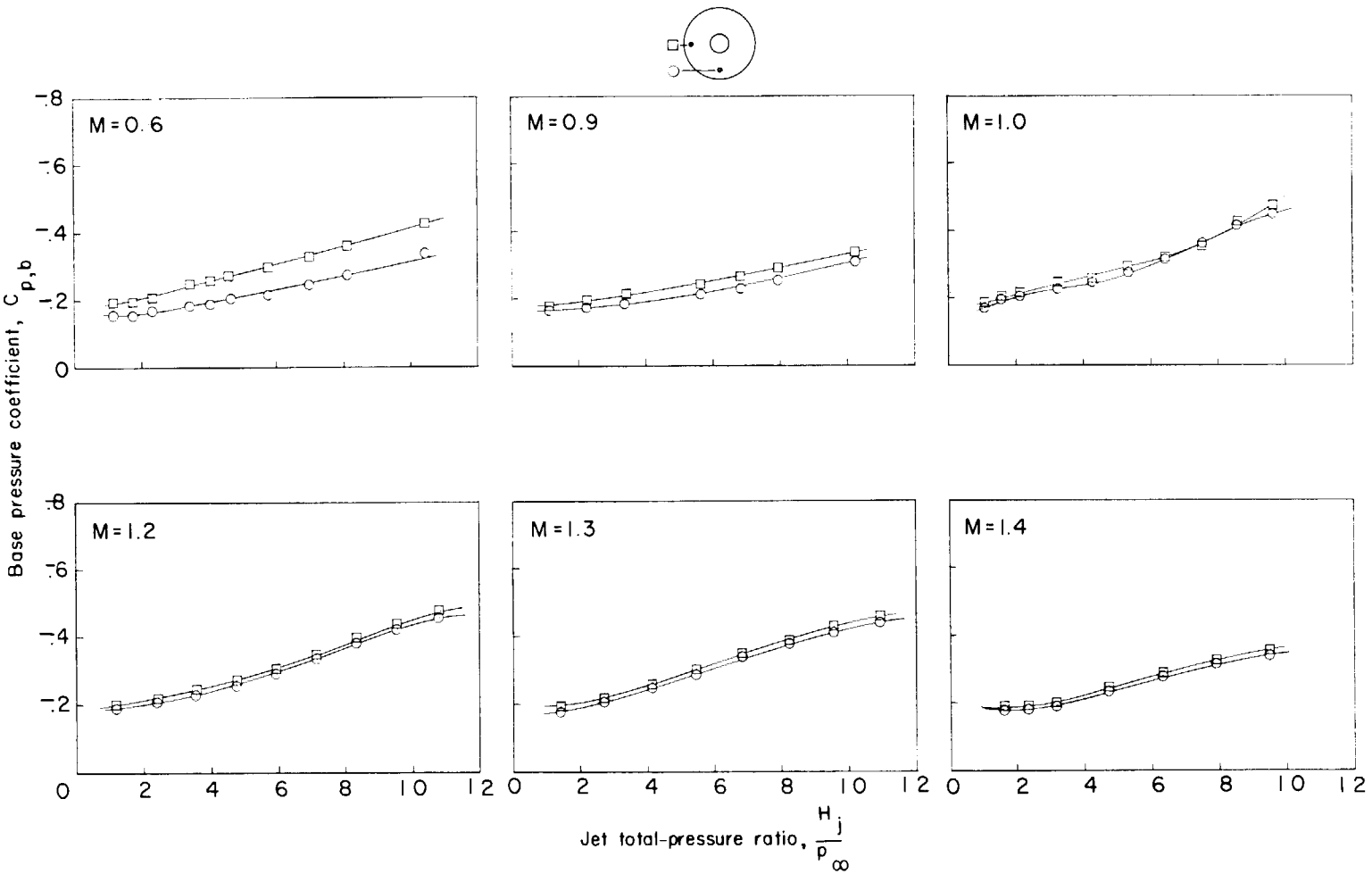

(a) $d_j/d_b = 0.225$.

Figure 3.- Effect of jet total-pressure ratio on base pressure coefficient of single-jet models.

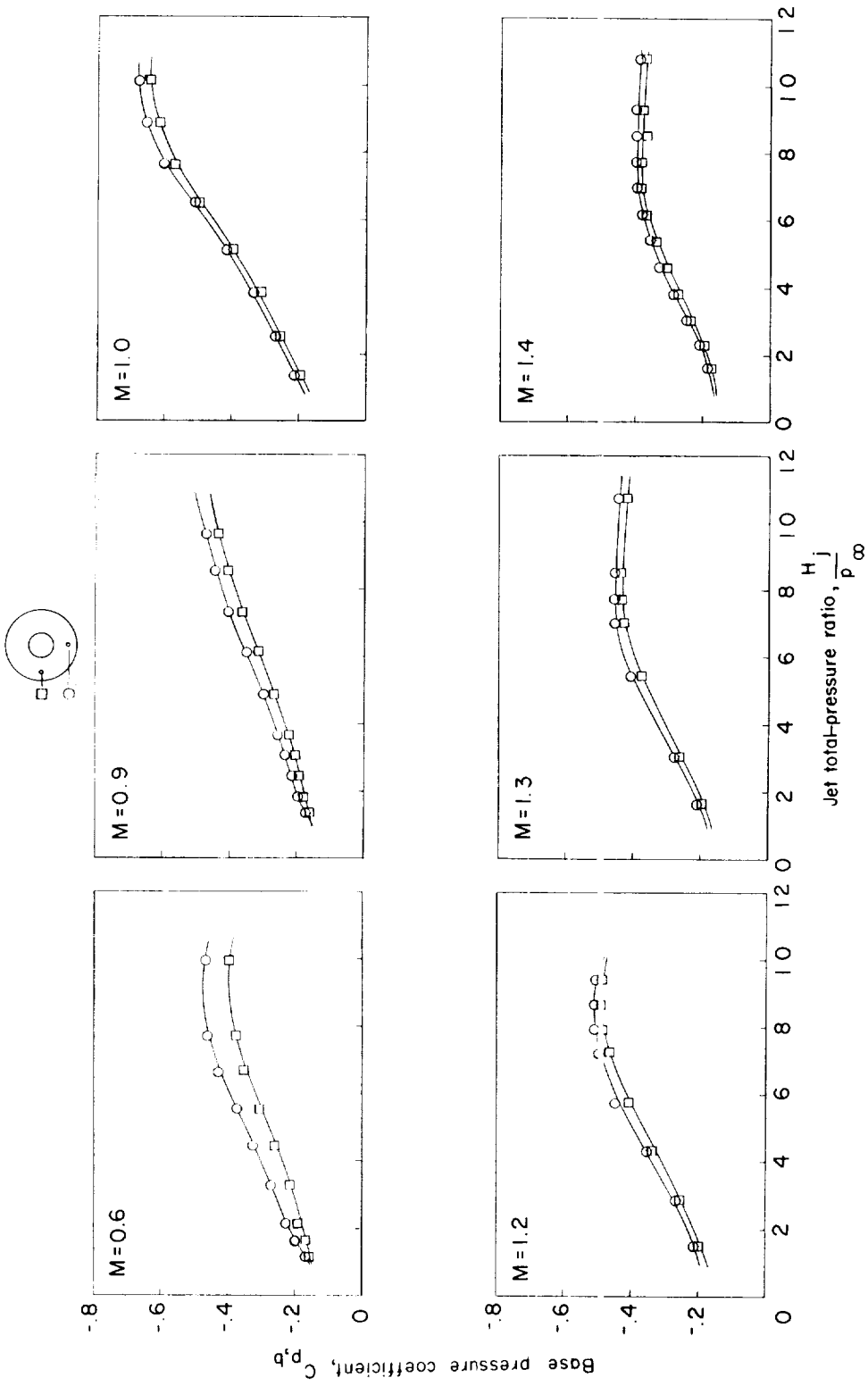

(b) $d_j/d_b = 0.320$.

Figure 3.- Continued.

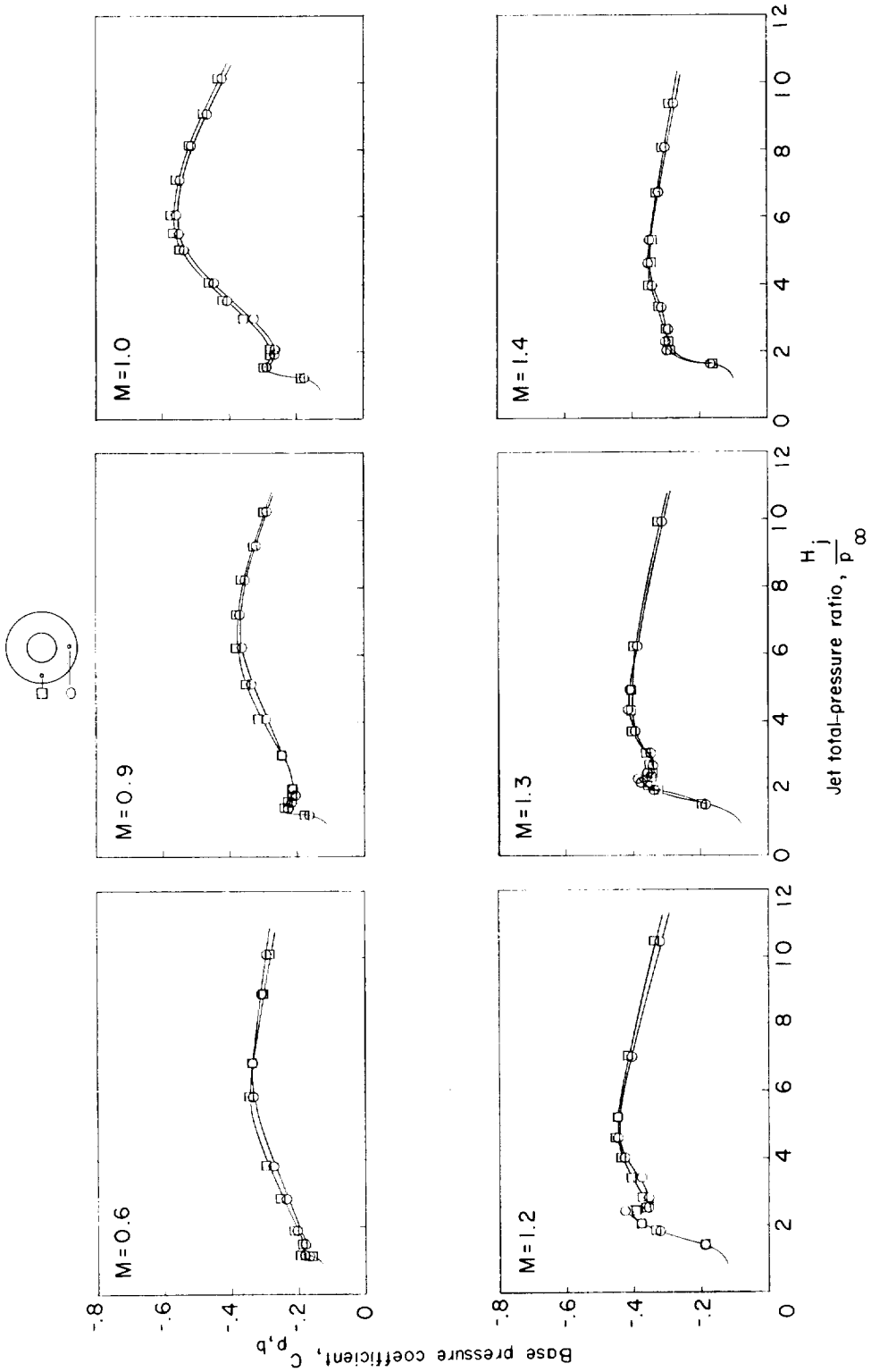

(c) $d_j/d_b = 0.450$.

Figure 3.- Continued.

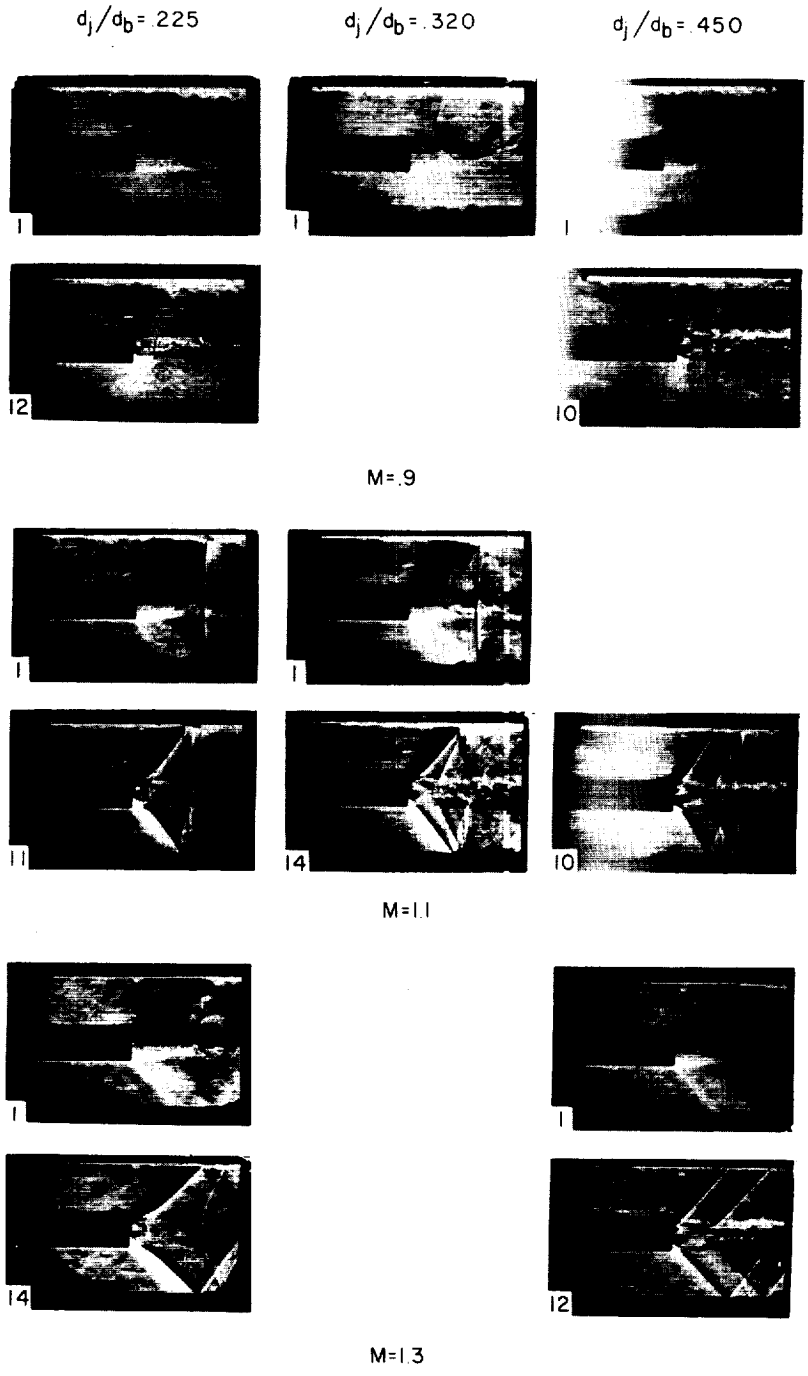

L-59-158

(d) Schlieren photographs for single jet. (Numerals in lower left-hand corner indicate jet total-pressure ratio.)

Figure 3.- Concluded.

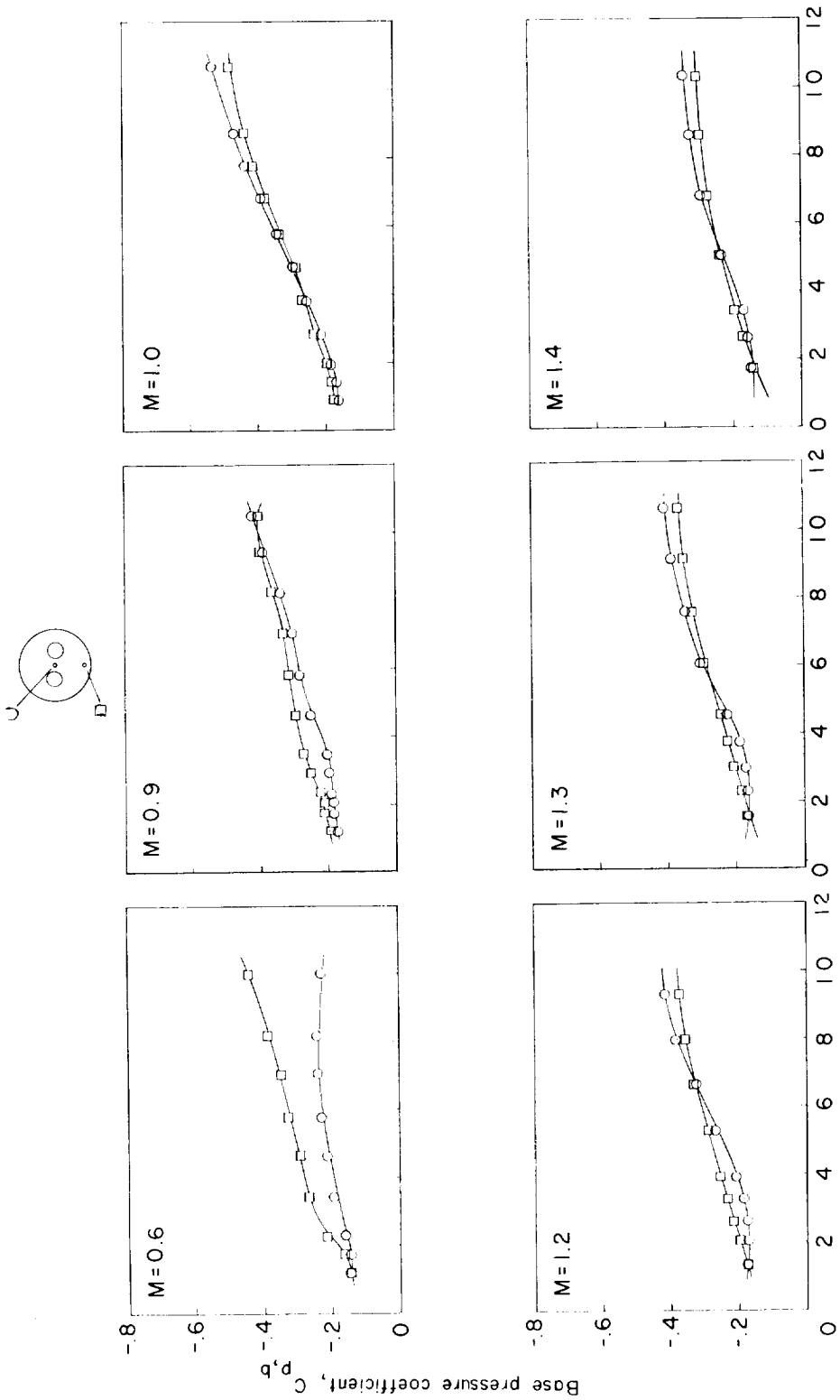

(a) $d_j/d_b = 0.155$.

Figure 4.- Effect of jet total-pressure ratio on base pressure coefficient of two-jet models.

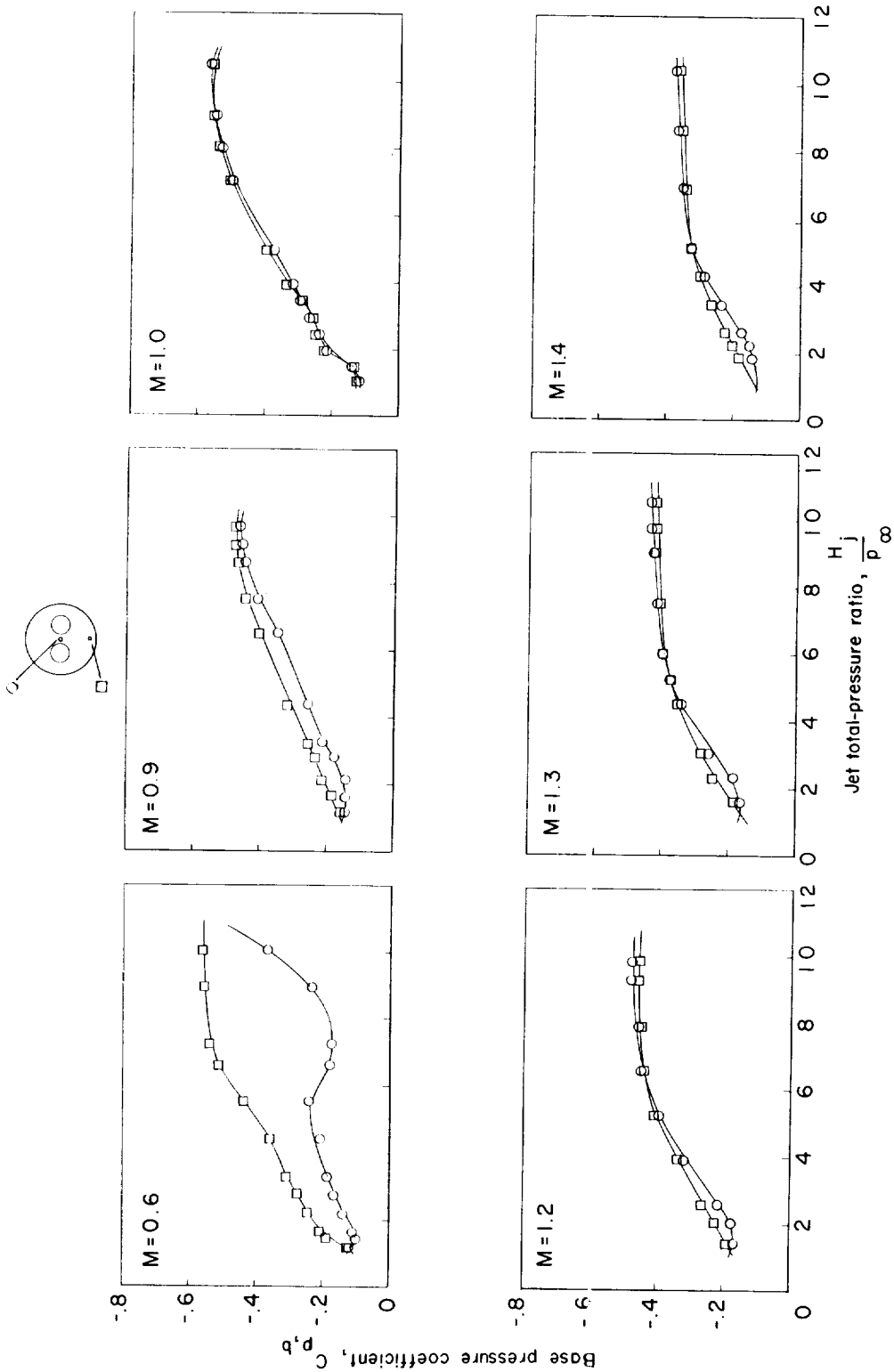

(b) $d_j/d_b = 0.225$.

Figure 4.- Continued.

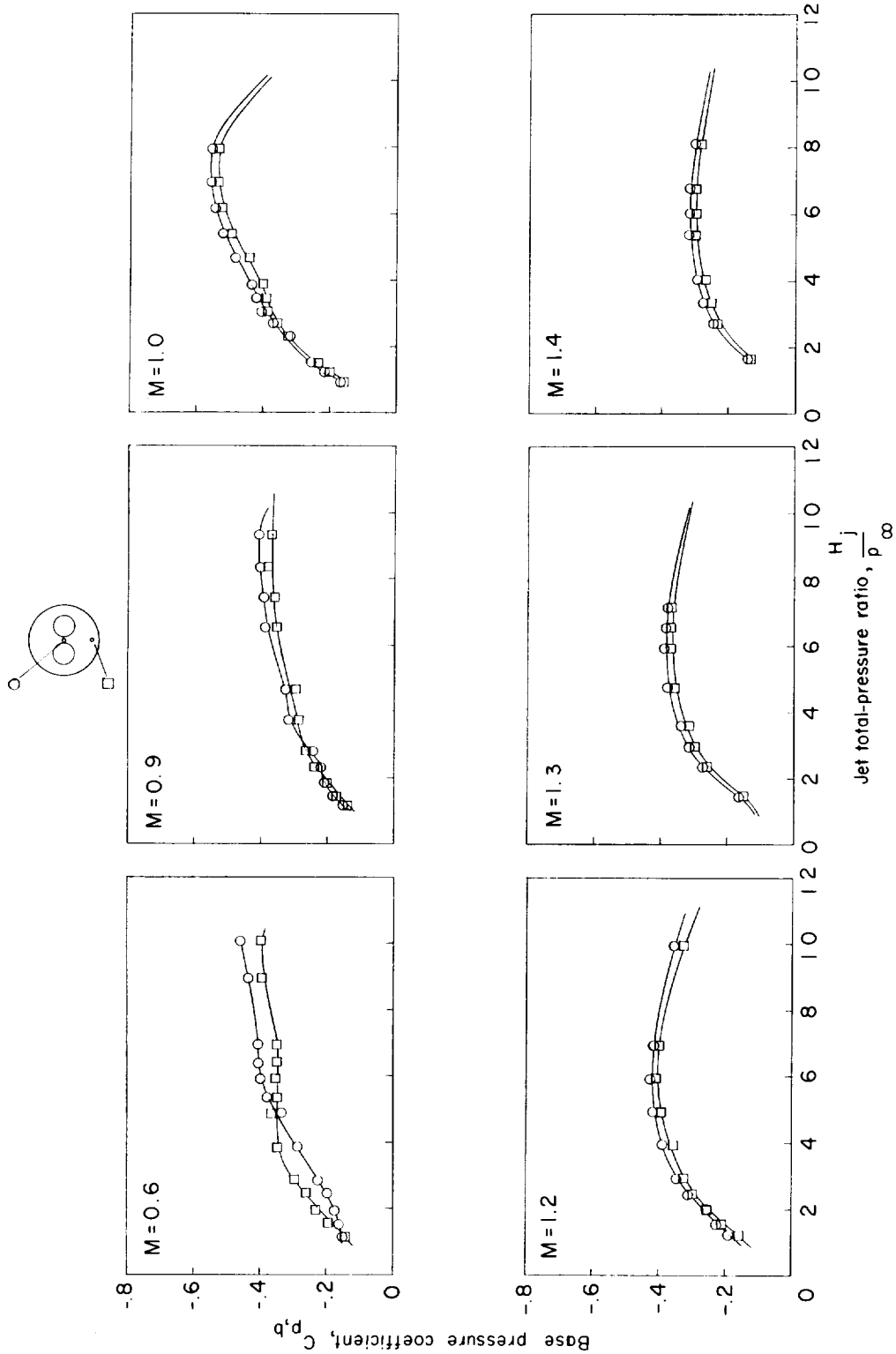

(c) $d_j/d_b = 0.320$.

Figure 4.- Continued.

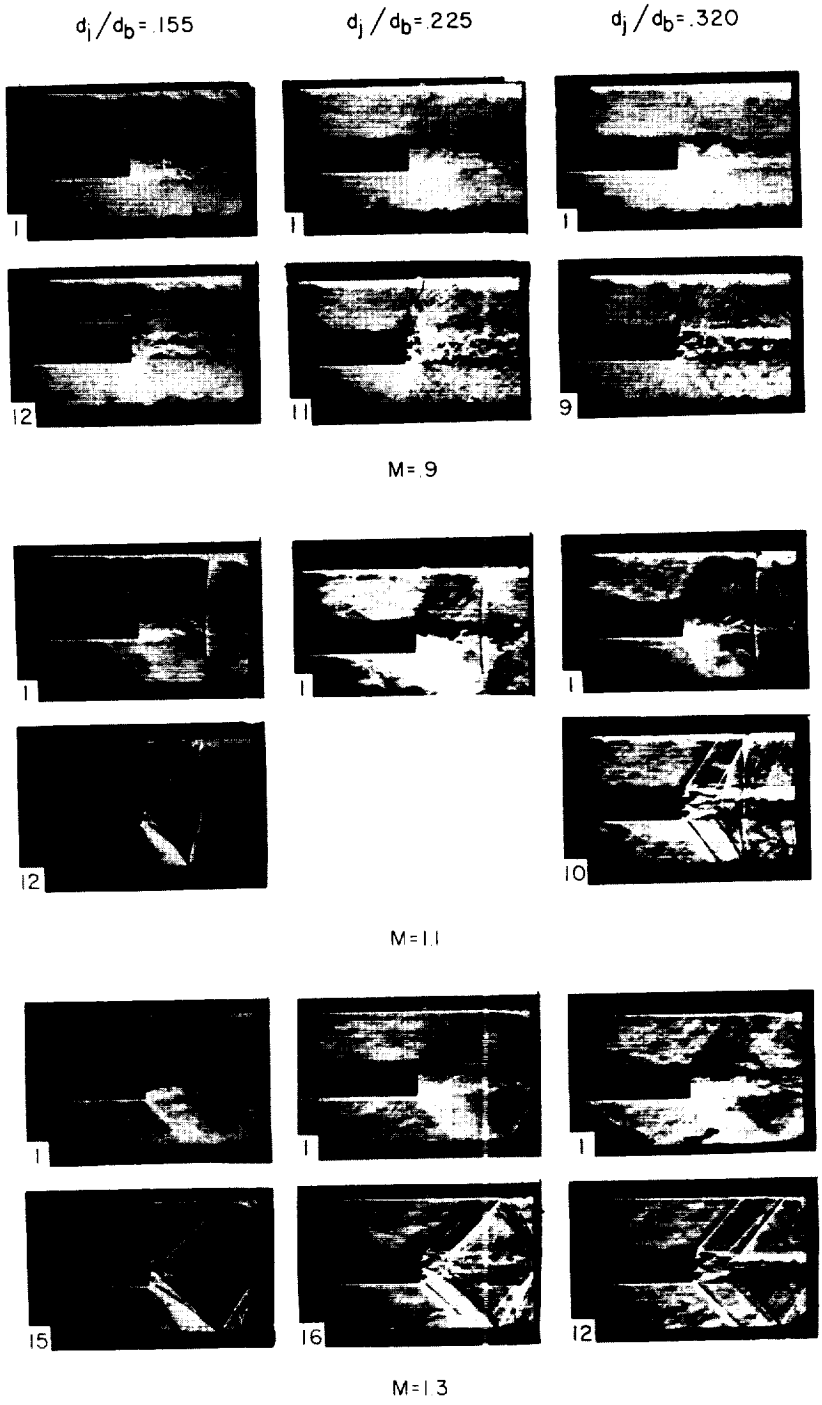

L-59-159

(d) Schlieren photographs for two jets. (Numerals in lower left-hand corner indicate jet total-pressure ratio.)

Figure 4.- Concluded.

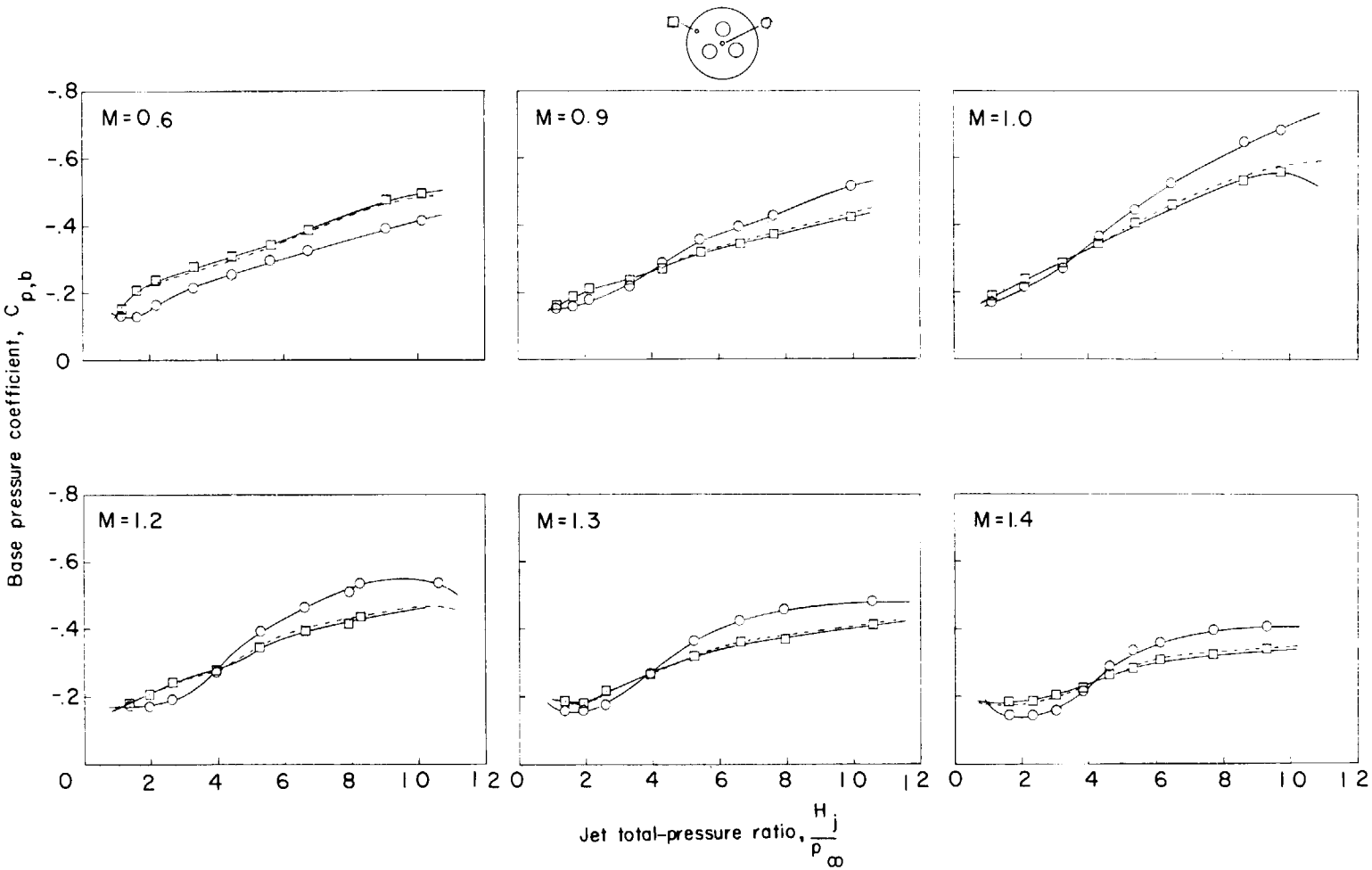

(a) $d_j/d_b = 0.155$.

Figure 5.- Effect of jet total-pressure ratio on base pressure coefficient of three-jet models.

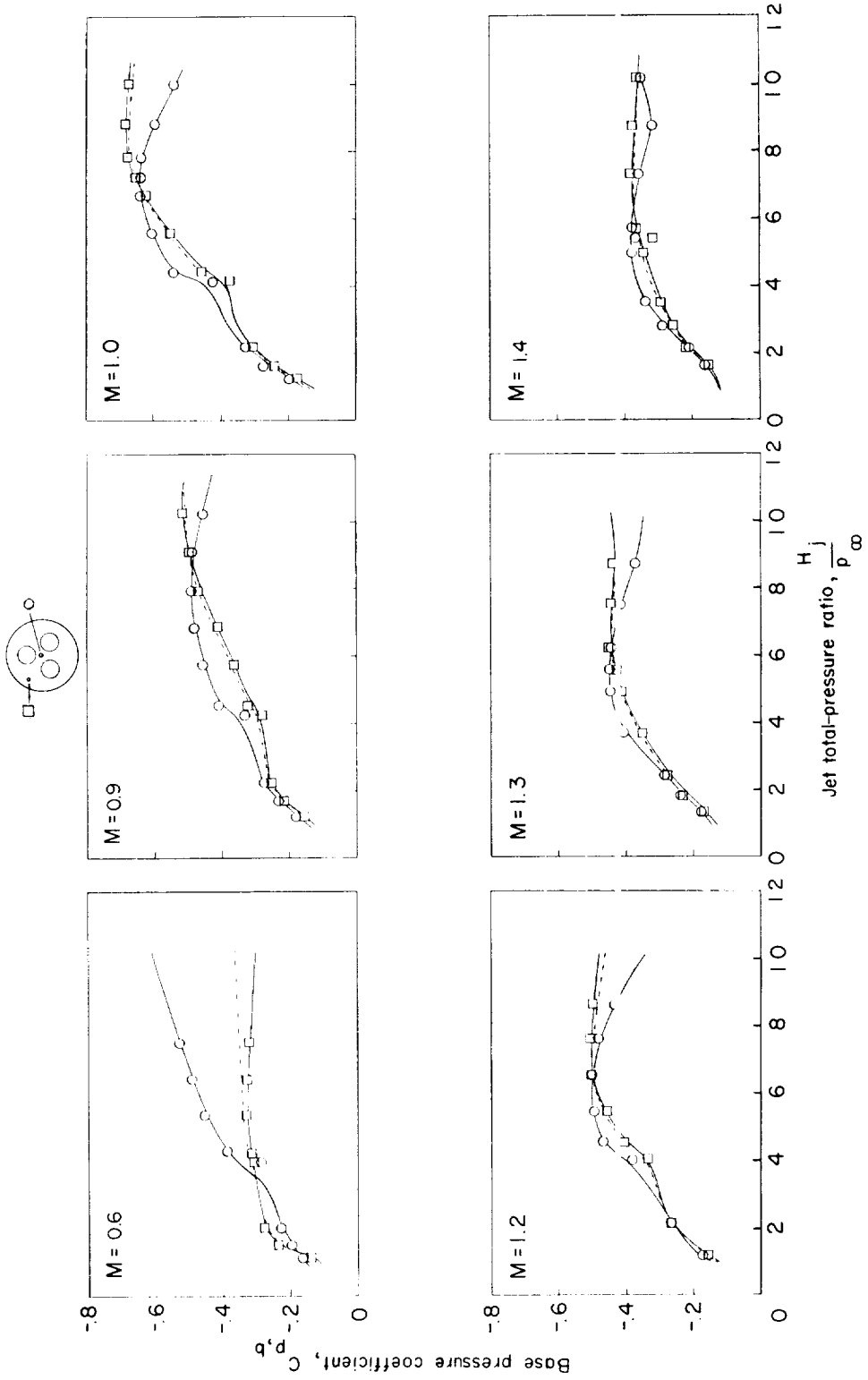

(b) $d_j/d_b = 0.225$.

Figure 5.- Continued.

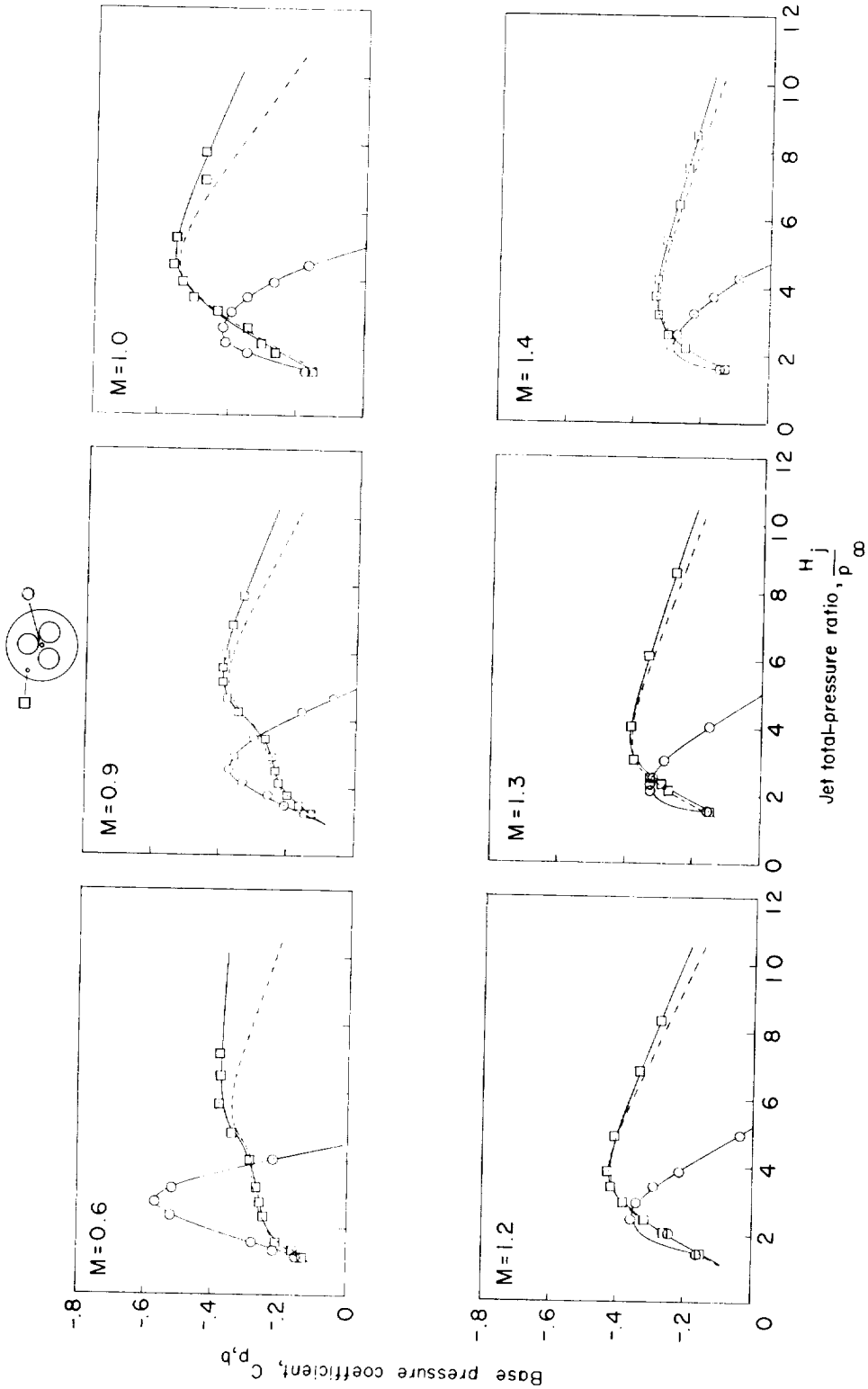

(c) $d_j/d_b = 0.320$.

Figure 5.- Continued.

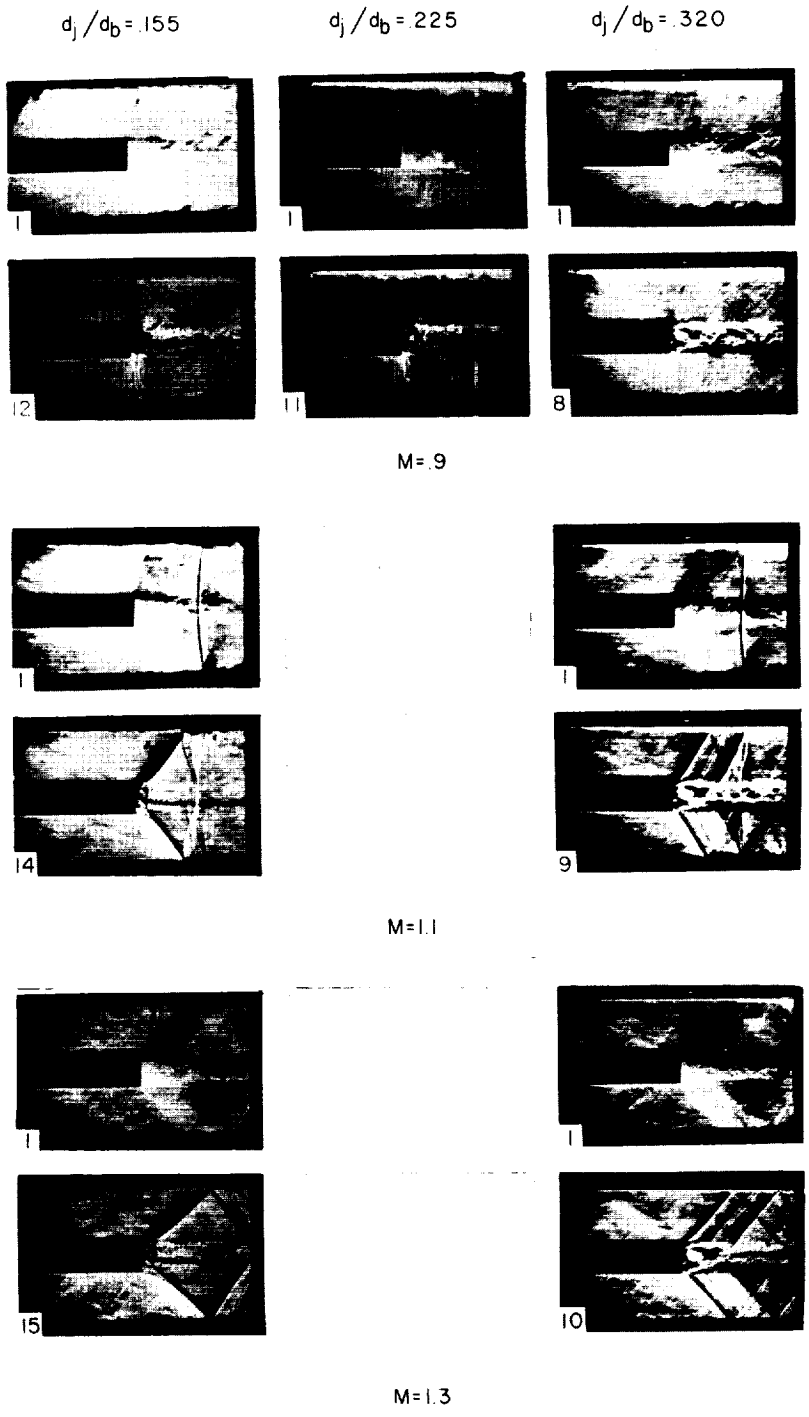

L-59-160

(d) Schlieren photographs for three jets. (Numerals in lower left-hand corner indicate jet total-pressure ratio.)

Figure 5.- Concluded.

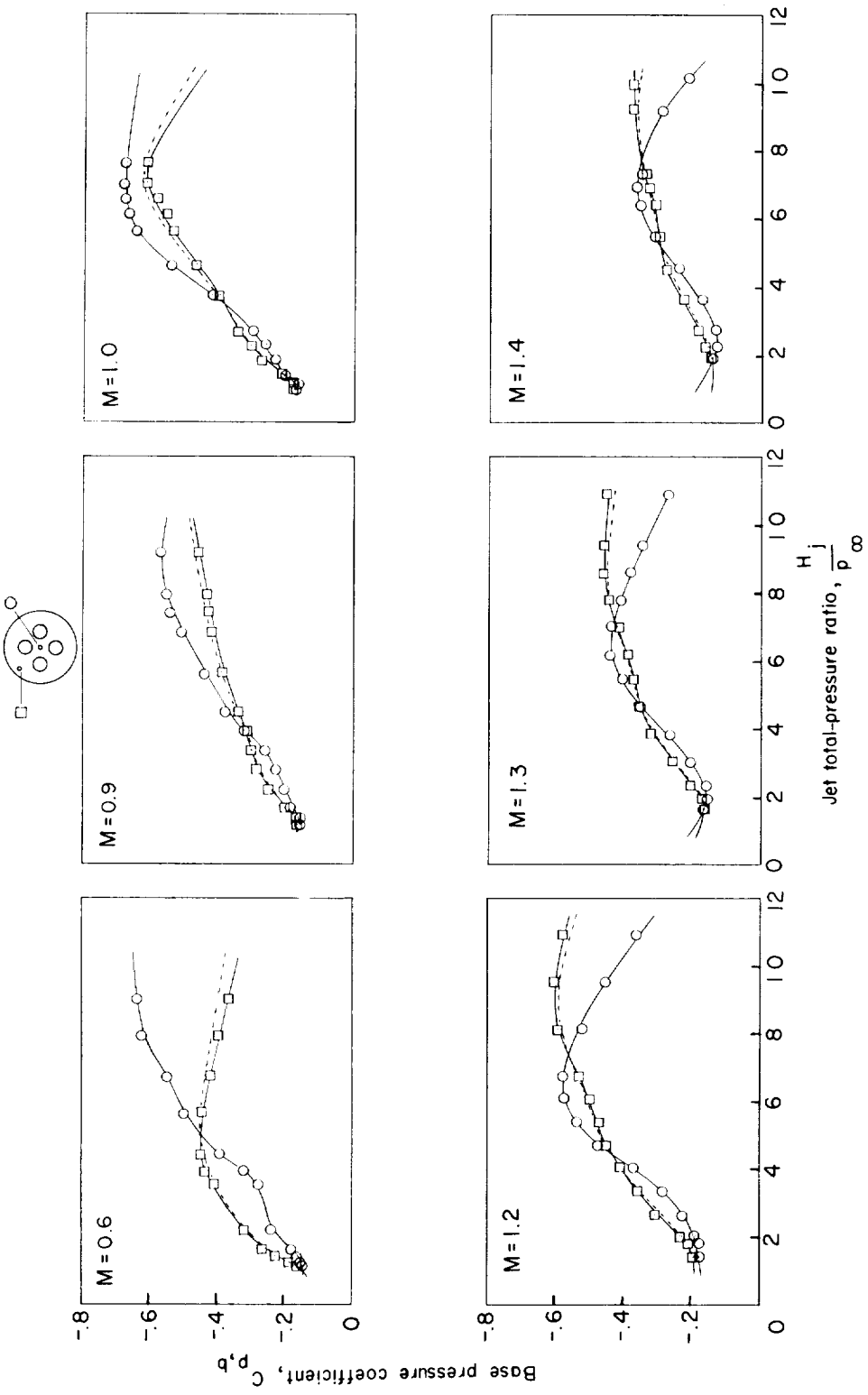

(a) $d_j/d_b = 0.155$.

Figure 6.- Effect of jet total-pressure ratio on base pressure coefficient of four-jet models.

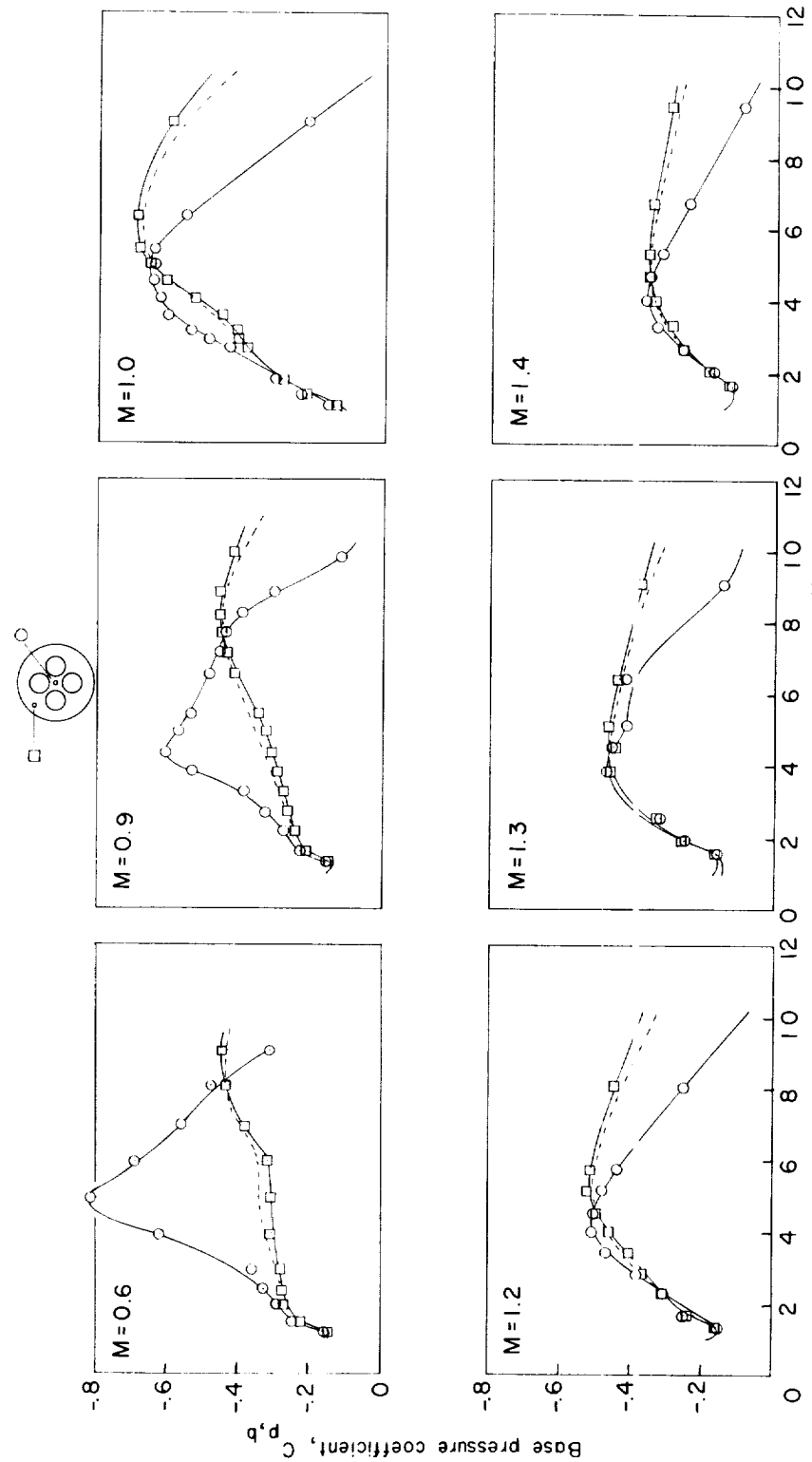

(b) $d_j/d_b = 0.225$.

Figure 6.- Continued.

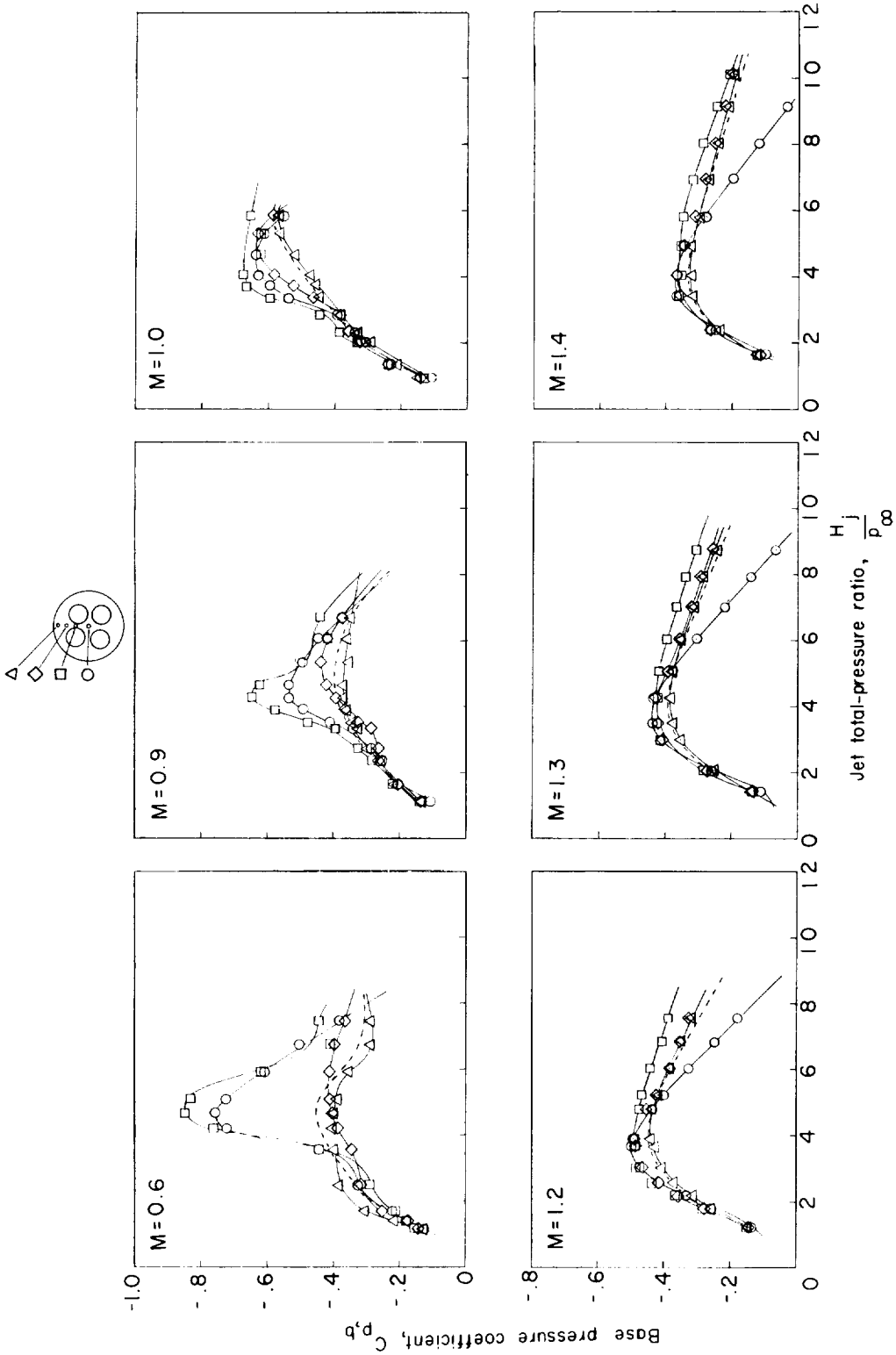

(c) $d_j/d_b = 0.278$.

Figure 6.- Continued.

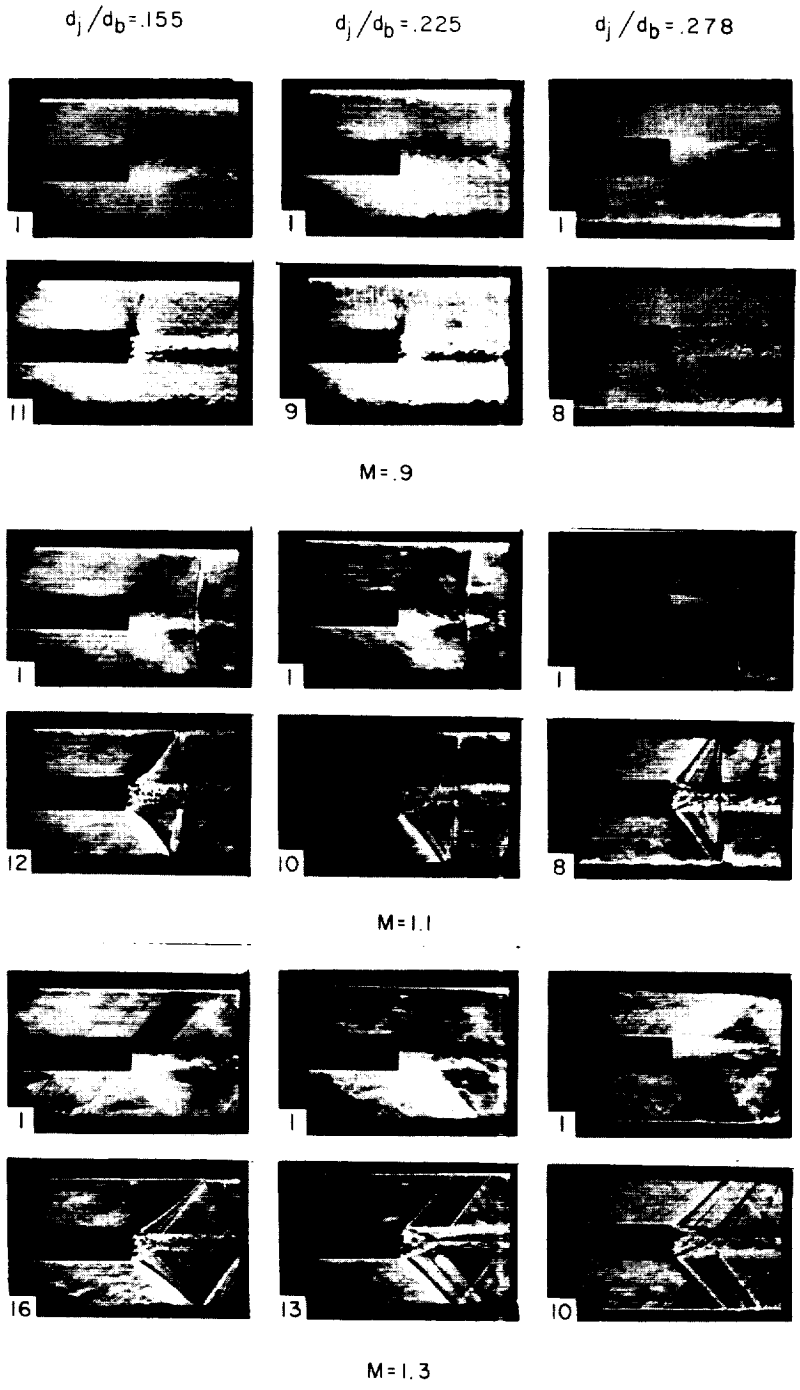

L-59-161

(d) Schlieren photographs for four jets. (Numerals in lower left-hand corner indicate jet total-pressure ratio.)

Figure 6.- Concluded.

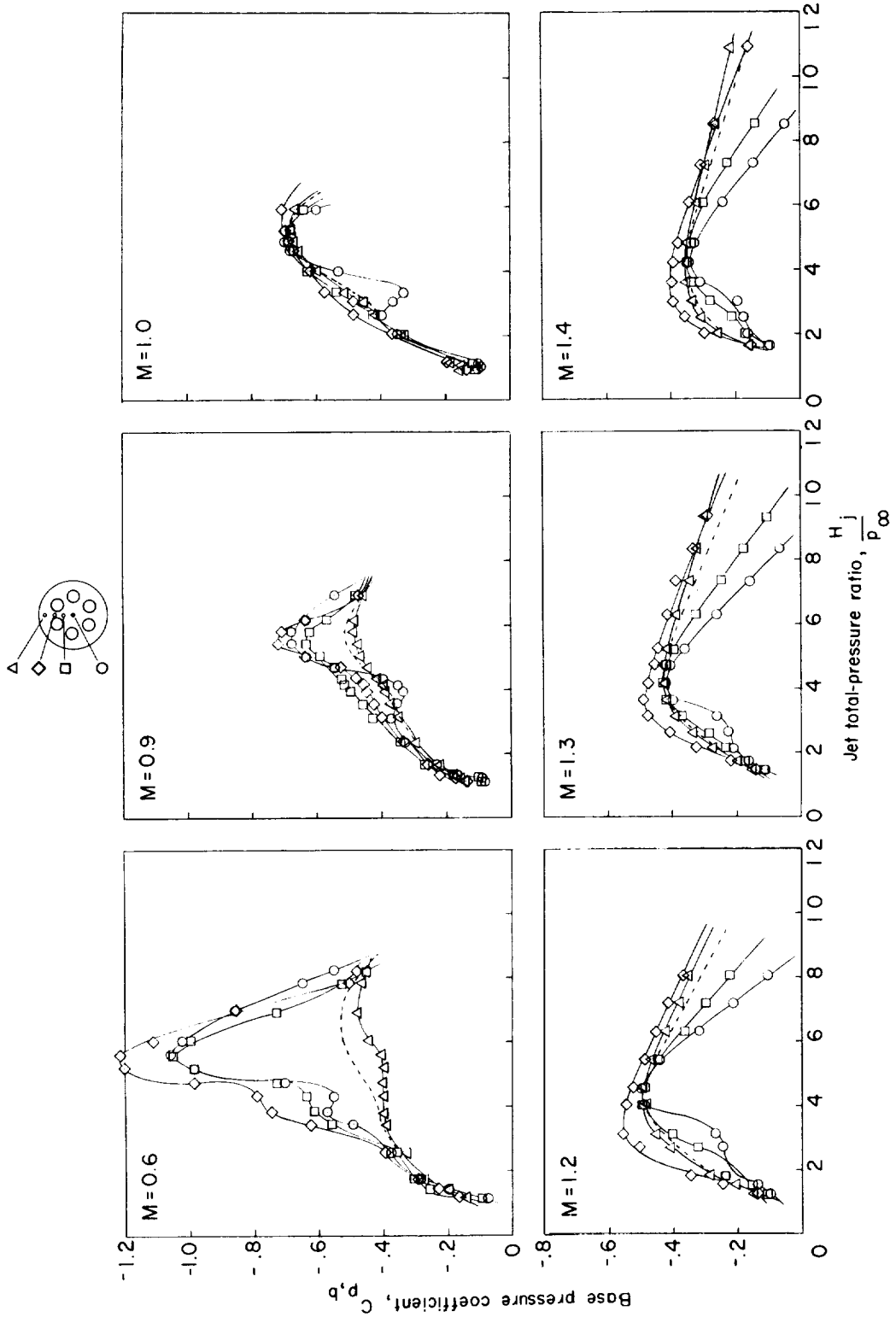

Figure 7.- Effect of jet total-pressure ratio on base pressure coefficient of six-jet model. $d_j/d_b = 0.225$.

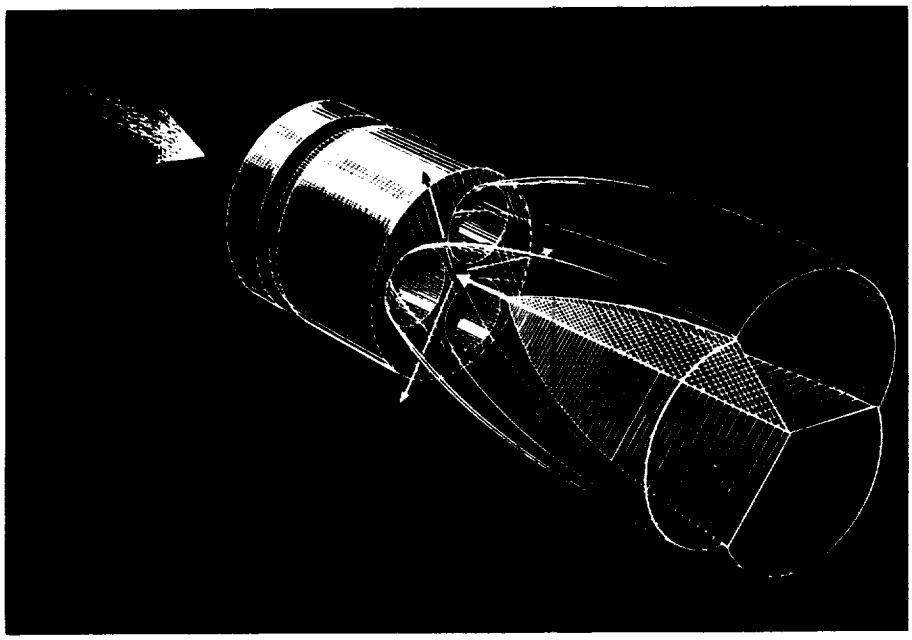

(a) Schematic drawing of nozzles exhausting at overpressure condition.

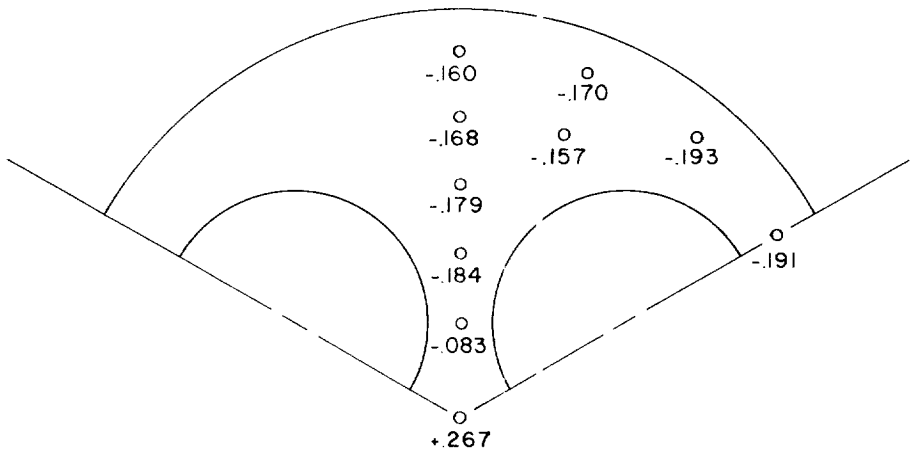

o— Indicates static pressure orifice location

The numbers represent base pressure coefficients measured at each orifice location for $H_j/p_\infty = 10.5$ and $M = 1.4$

(b) Pressure-coefficient distribution on model base.

Figure 8.- Effect of mutual jet interference on the three-jet model. $d_j/d_b = 0.320$.

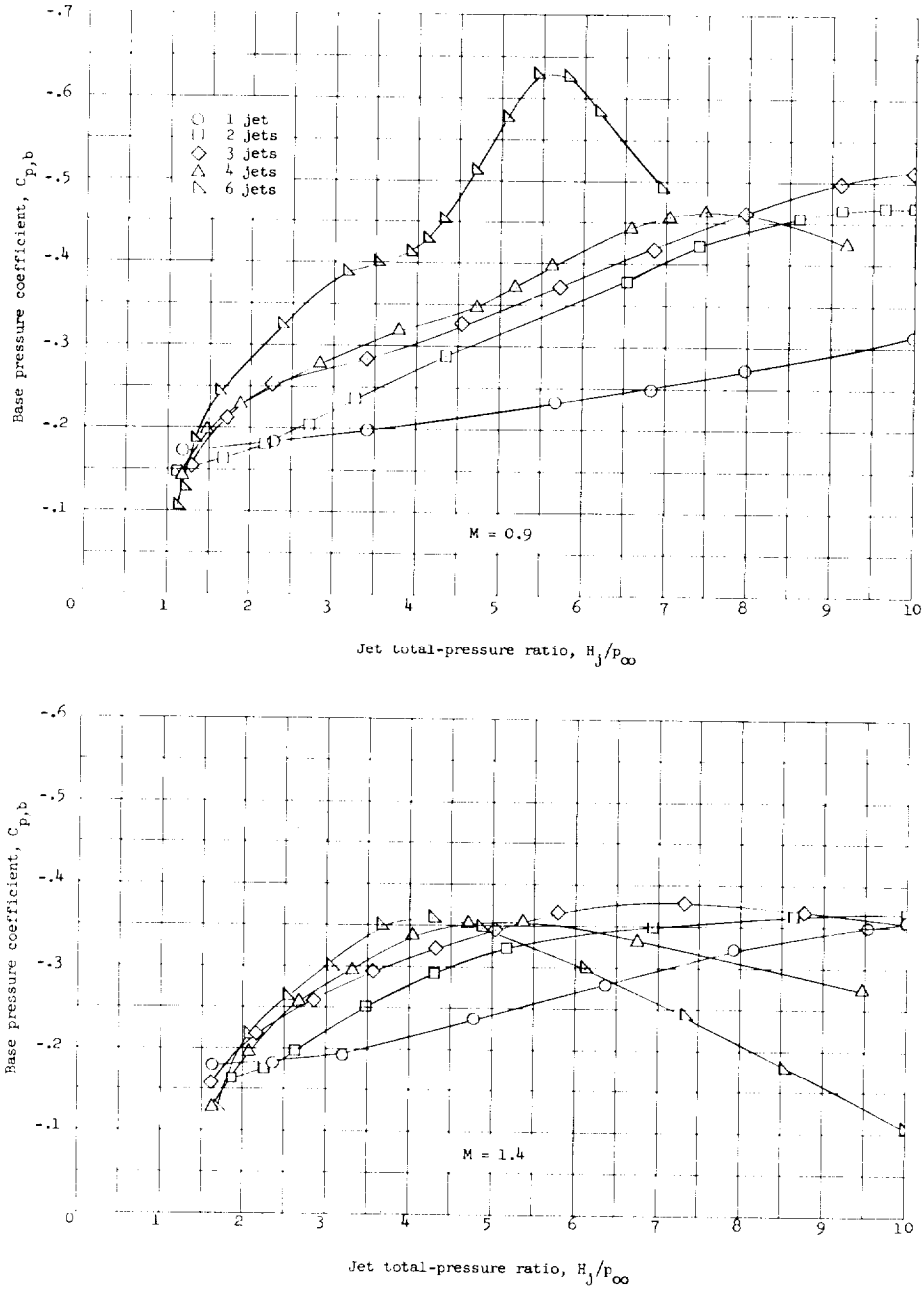

Figure 9.- Typical curves showing the effect on base pressure coefficient of varying the jet total-pressure ratio and number of jets. $d_j/d_b = 0.225$ for each jet. (Base pressure coefficients were calculated using the pressures measured at the outboard orifice location.)

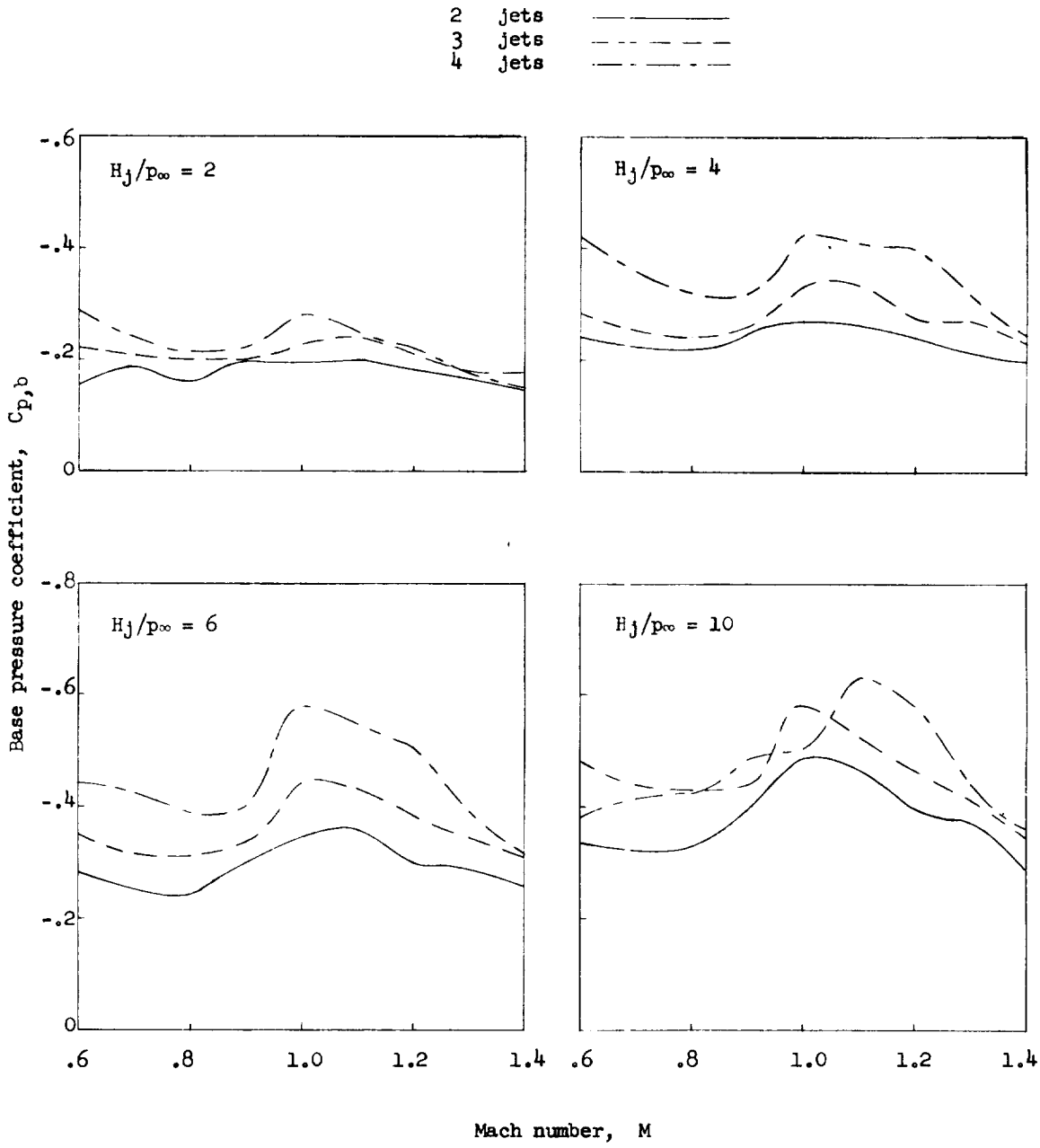

(a) $d_j/d_b = 0.155$.

Figure 10.- Effect of number of jets on the base pressure coefficient at constant jet-to-base diameter ratios over the Mach number range.

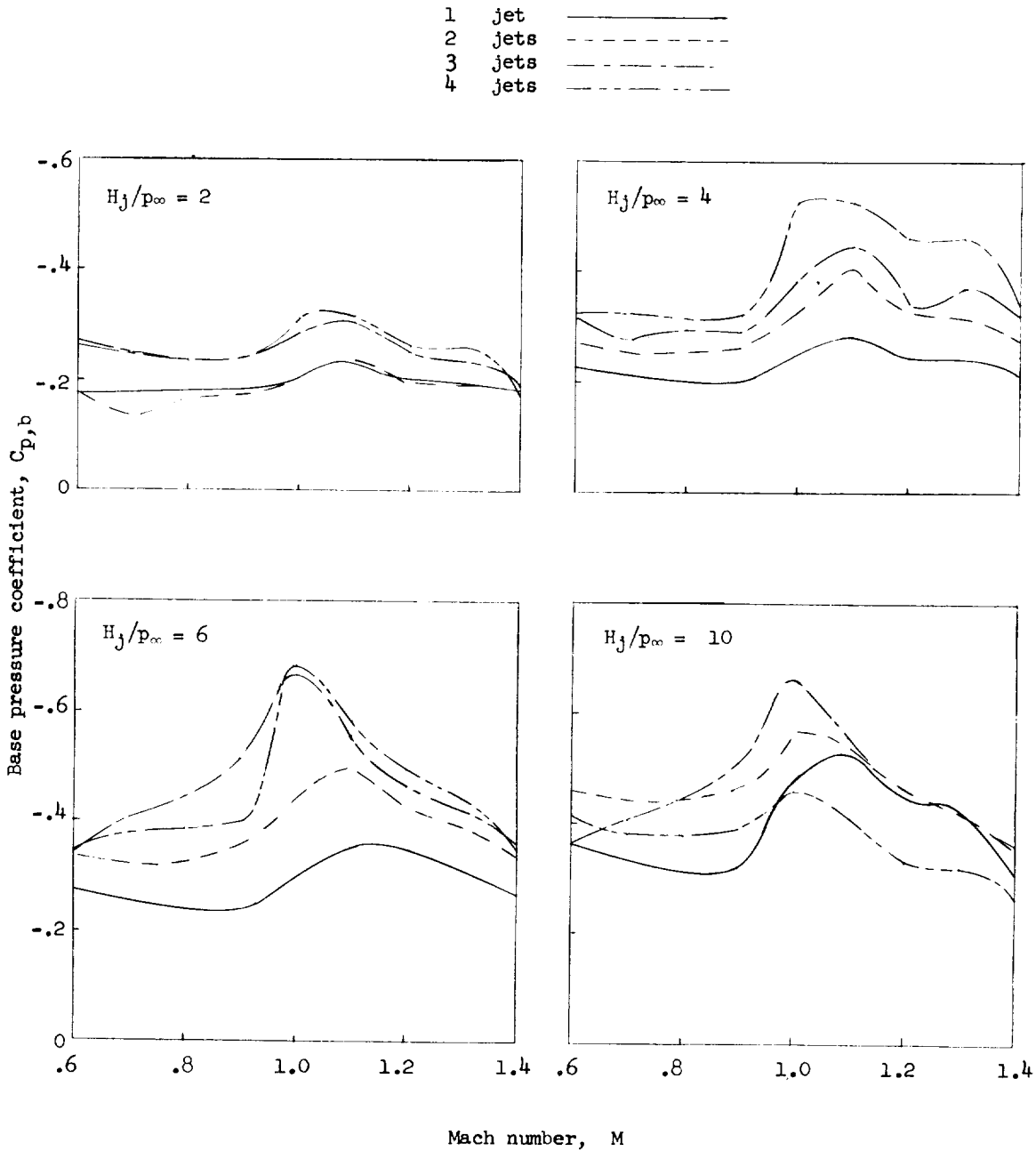

(b) $d_j/d_b = 0.225$.

Figure 10.- Continued.

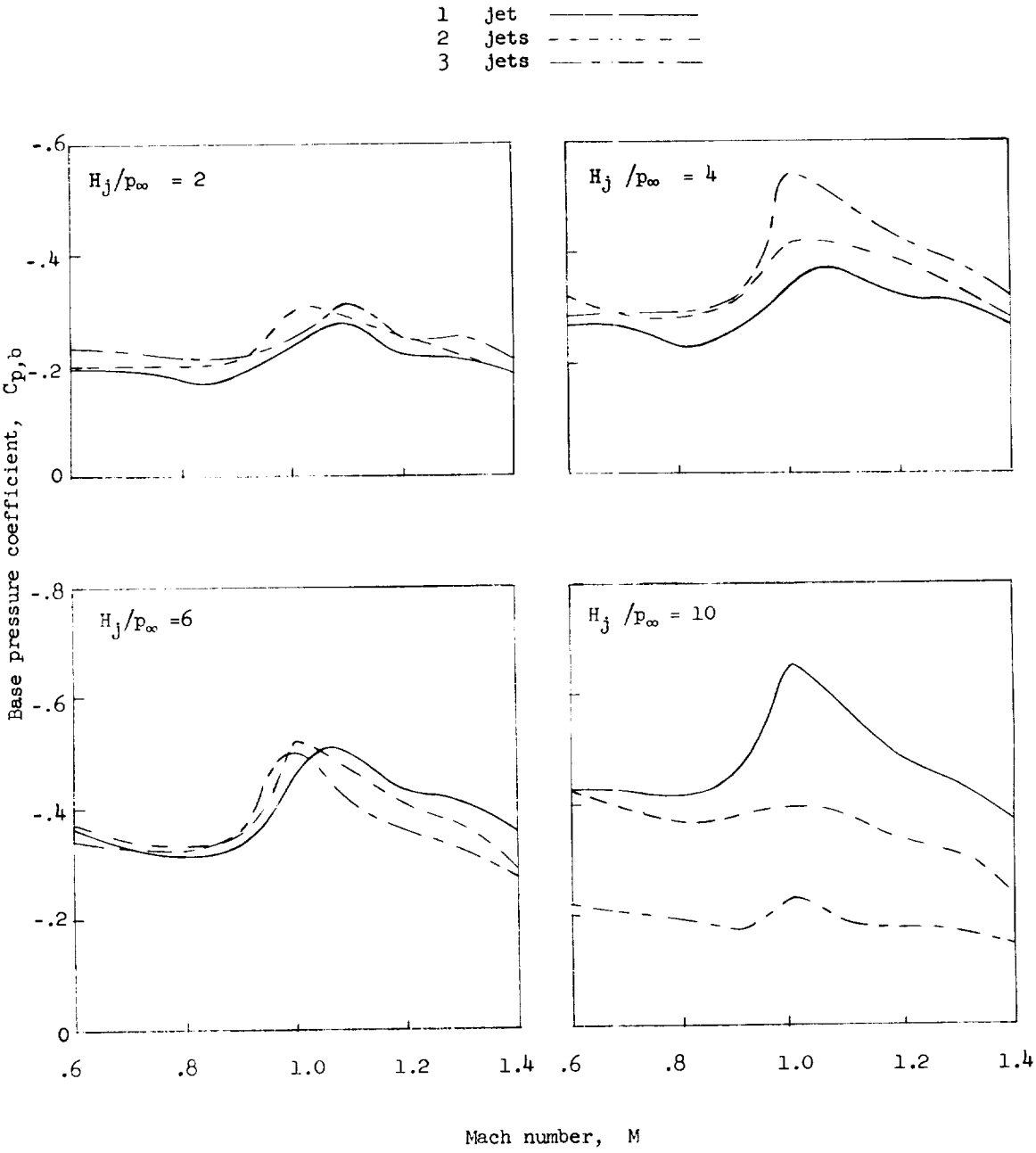

(c) d_j/d_b = 0.320.

Figure 10.- Concluded.

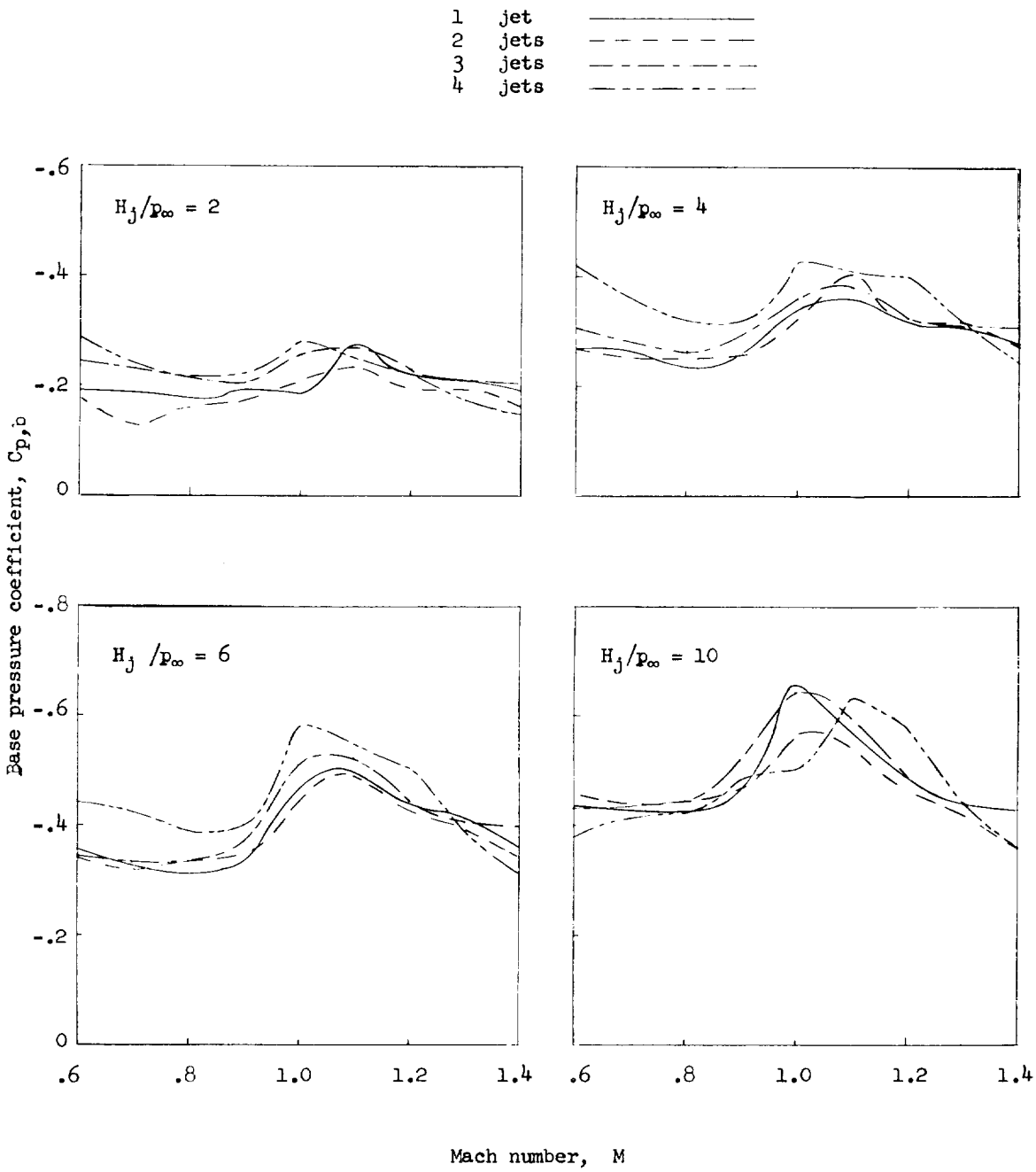

(a) $A_j/A_b = 0.102$.

Figure 11.- Effect of number of jets on the base pressure coefficient at constant jet-to-base area ratios over the Mach number range.

Figure 12.- Contour plots showing base pressure coefficient as a function of jet-to-base diameter ratio and jet total-pressure ratio.

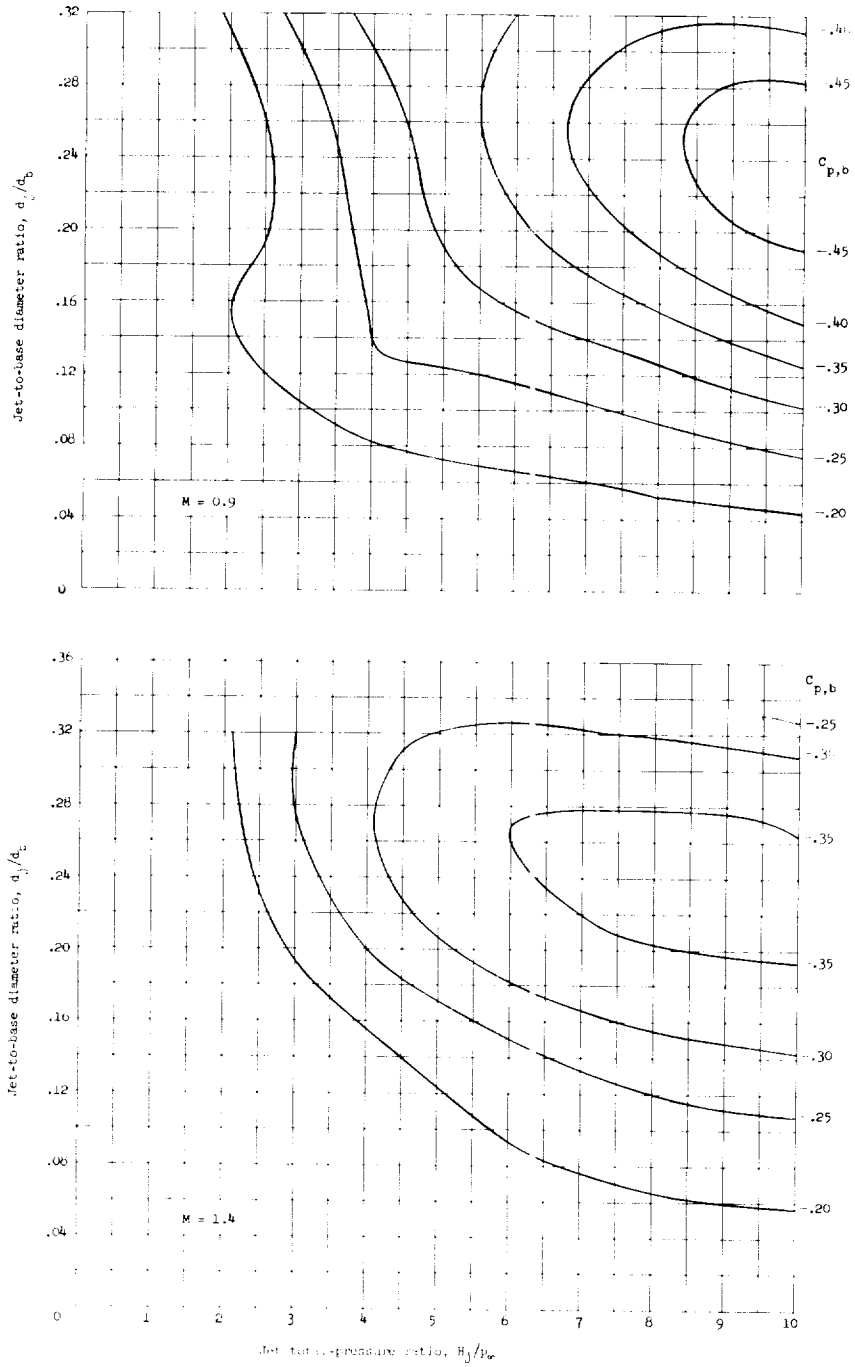

(b) Two jets.

Figure 12.- Continued.

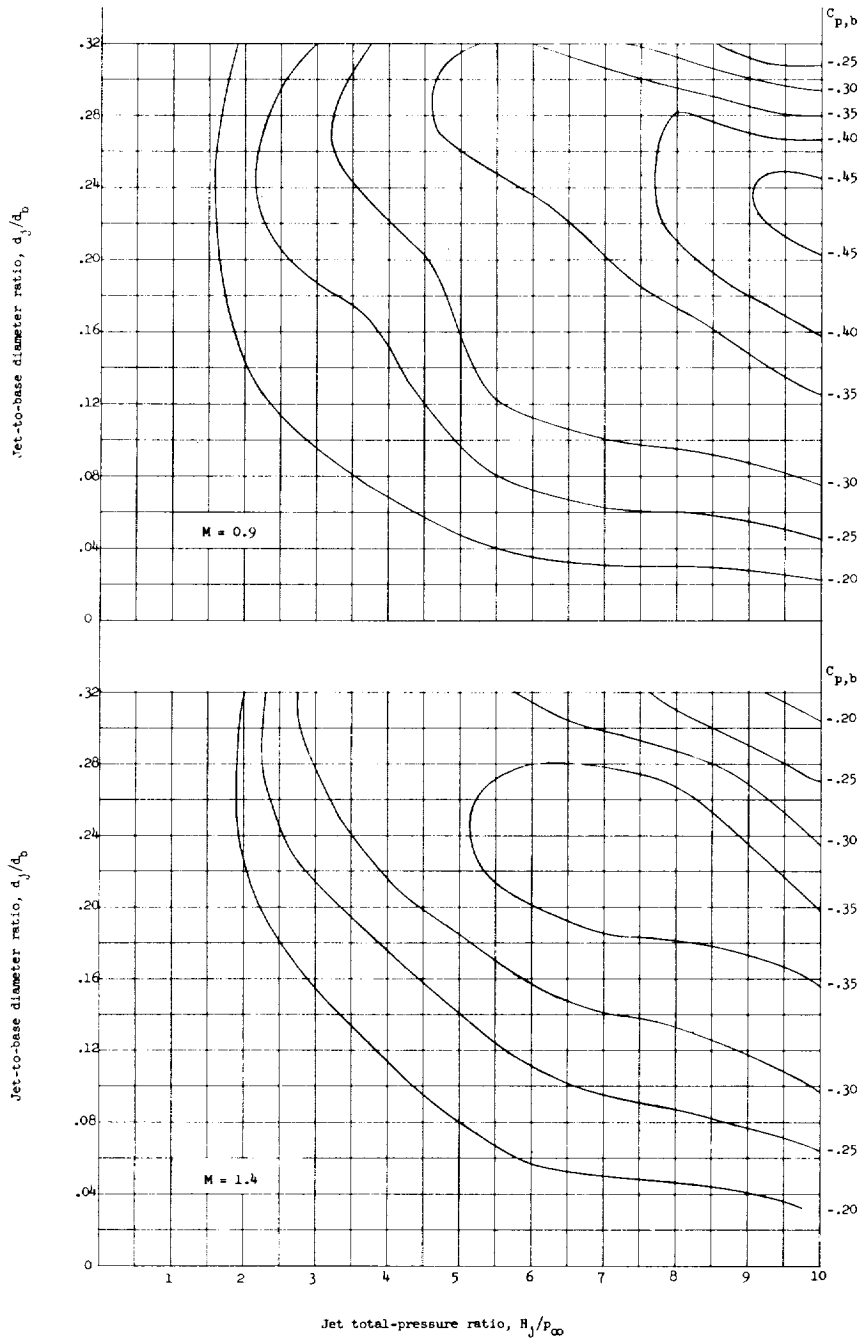

(c) Three jets.

Figure 12.- Continued.

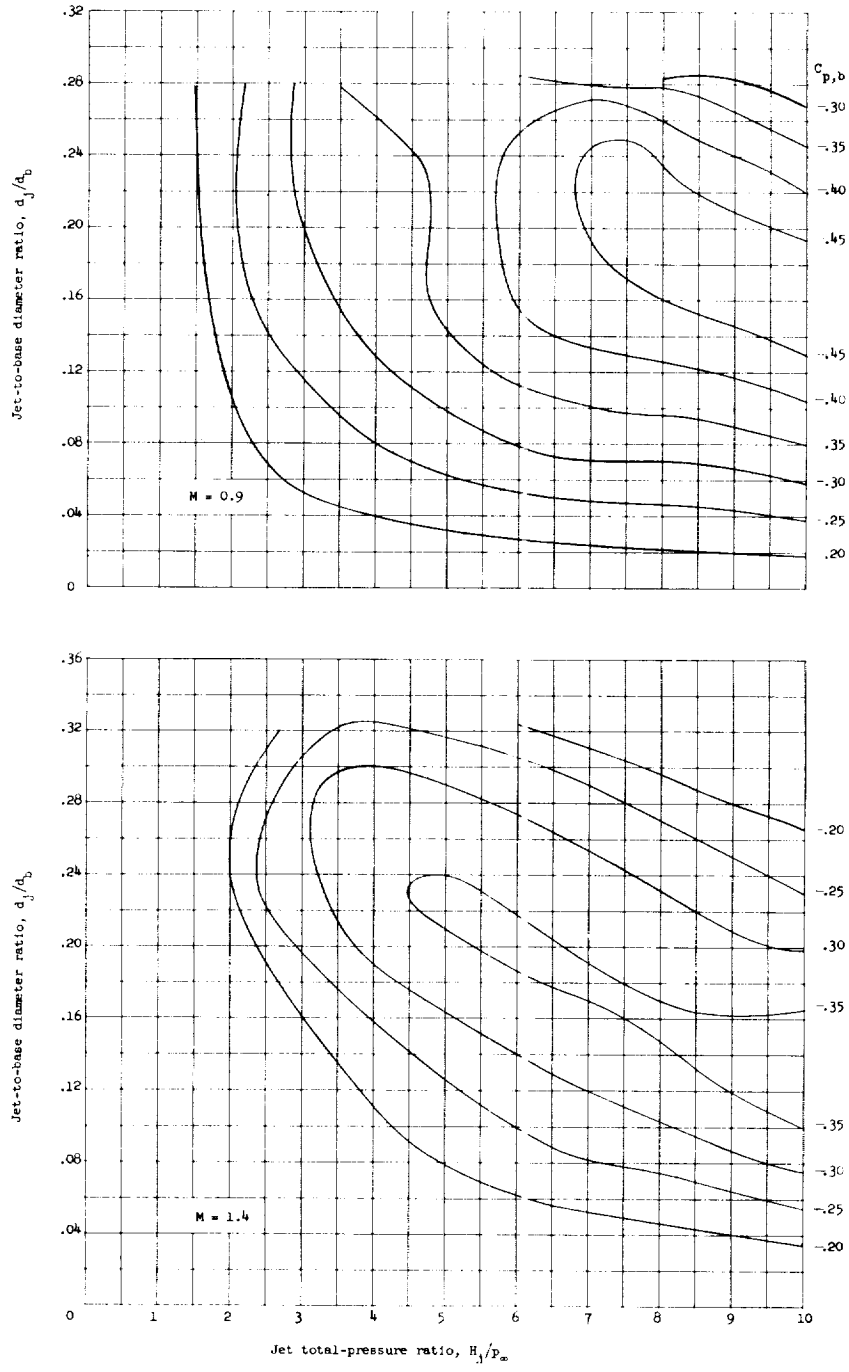

(d) Four jets.

Figure 12.- Concluded.